AN ABSTRACT OF THE THESIS OF

Wesley von Dassow for the degree of Master of Science in Geology presented on 23 March, 2018.

Title: Geomorphic Evidence for Differential Rock Uplift Across the Southern Cascadia Forearc.

Abstract approved:

_____

Eric Kirby

The nature of upper plate deformation along the Cascadia subduction zone (CSZ) is poorly understood. Systematic covariation among topographic relief, geodetically determined uplift rates, decadal to millennial erosion rates, and the frequency of episodic tremor and slip (ETS) along the Cascadia forearc suggest a genetic association between forearc topography and plate boundary deformation. Although spatial variations in uplift are commonly attributed to the inboard position of the locked plate interface, the association of high topographic relief and rapid erosion across the boundary between the central Oregon Coast Ranges and the Klamath mountains suggests that ongoing rock uplift may contribute to this signal. Here, I test this hypothesis using a combination of stream profile analysis, observations of fluvial terraces, and existing determinations of watershed-average erosion rate. In the Rogue River watershed, these analyses reveal systematic spatial patterns in channel steepness (a measure of channel gradient normalized for contributing basin area) that delineate a western block characterized by high channel

steepness and high local relief (up to 1.5 km) from an eastern portion characterized by lower relief and gentler channels. The boundary between these two domains is a sharp, linear mountain front that trends NNE and is approximately coincident with a bedrock fault zone within the Western Klamath Terrane. East of this structure, herein referred to as the Eight Dollar Fault, fluvial networks are characterized by low-gradient, alluviated valleys, whereas western channels are decorated with flights of strath terraces and perched gravels attesting to recent incision. Longitudinal profiles of the trunk streams of the Rogue and Illinois Rivers exhibit a broad steepening across this transition that is manifest as a convex longitudinal profile. Knickpoints are observed throughout the watershed, but are not systematically associated with the elevation or drainage area of the convexities along trunk channels. Comparison of channel steepness values to existing data on erosion rate suggest that these differences in landscape morphology, channel profile steepness, and geomorphic character of channels are associated with sustained high rates of rock uplift and erosion in the western Klamath mountains. These results suggest that the western Klamath mountains are actively uplifting relative to the eastern forearc. Permanent strain associated with active deformation within the southern Cascadia forearc may be a non-negligible component geodetically measured uplift rates in the region.

Geomorphic Evidence for Differential Rock Uplift Across the Southern Cascadia
Forearc

by
Wesley von Dassow

A THESIS

submitted to

Oregon State University

in partial fulfillment of
the requirements for the
degree of

Master of Science

Presented 23 March, 2018
Commencement June 2019

Master of Science thesis of Wesley von Dassow presented on 23 March, 2018

APPROVED:

_____

Major Professor, representing Geology

_____

Dean of the College of Earth, Ocean, and Atmospheric Sciences

_____

Dean of the Graduate School

I understand that my thesis will become part of the permanent collection of Oregon State University libraries. My signature below authorizes release of my thesis to any reader upon request.

_____

Wesley von Dassow, Author

TABLE OF CONTENTS

TABLE OF CONTENTS (Continued)

LIST OF FIGURES

LIST OF TABLES

1. INTRODUCTION

The origin and support of topography along the Cascadia forearc remains an outstanding question in the tectonic evolution of the active margin of western North America. The Coast Ranges are a forearc topographic high that extends the length of the Cascadia subduction zone. Topographic relief along the Coast Ranges varies significantly along the plate margin (Kelsey et al., 1994), from high relief in the Olympic Mountains, through a low in southern Washington and central Oregon, to high relief again in the Klamath-Siskiyou ranges of southern Oregon and northern California (Figure 1). These variations in topographic relief exhibit strong correspondence with the lithospheric architecture of North America and with the age and roughness of the subducting Juan de Fuca and Gorda plates suggesting that (McNutt, 1983; Kelsey et al., 1994). Moreover, the co-variance of geodetic uplift rates (Burgette et al., 2009) and the frequency of episodic tremor and slip along the plate interface (Brudzinski and Allan, 2007) suggest the possibility of a dynamic link between topography and plate boundary deformation (e.g., Willett, 1999).

Evaluating permanent strain within the Cascadia forearc is made challenging by the relatively few recognized active faults (Figure 2), the rugged terrain, and the heavy vegetative canopy. Moreover, most known or suspected active faults in the central and northern forearc trend E-W, orthogonal to the topographic trend of the Coast Ranges (Blakely et al., 2000), Puget Sound (Nelson et al., 2003; Blakely et al., 2002), and Vancouver Island region (Morell et al., 2017; Delano et al., 2017). In the southern Cascadia forearc, faults recognized as active are restricted to relatively minor reverse structures along the coast (Kelsey, 1990; USGS Quaternary Fault and Fold Database,

2006; Figure 2). Backarc deformation along strike-slip and normal faults in the Klamath Lake region (Meigs and Waldien, 2013; Speth et al., 2018) appears to be related to transtensional deformation associated with the western margin of the Basin and Range province.

Here, I evaluate permanent deformation in southern Cascadia through detailed topographic and stream profile analysis of the channel network in the Rogue River watershed. Previous analyses of the tectonic geomorphology of the Cascadia Coast Ranges focused on the central Oregon block (e.g., Kobor and Roering, 2004; Van Laningham et al., 2006), where contrasts in lithologic substrate between marine sedimentary rocks and basaltic volcanic rocks influence channel profile form. In contrast, the forearc region in the Klamath Mountains is underlain by a range of accreted terranes of Mesozoic age that host lithologies ranging from marine sedimentary rocks, arc volcanic sequences, accretionary mélange, ophiolites, and granitoids (Irwin, 1994). Despite this variability in substrate, the modern topography exhibits a distinct east-west dichotomy in mean elevation, local topographic relief, and channel steepness. Differences in these characteristics are coincident with a pre-existing fault system within the Western Klamath Terrane (Blake et al., 1985), suggesting that this structural weakness may be actively accommodating upper plate deformation in the southern Cascadia forearc.

2. BACKGROUND

2.1 Tectonostratigraphic Architecture of the Cascadia Forearc

The inner forearc region along the Cascadia subduction zone in northern California and Oregon is underlain by two tectonostratigraphic provinces, the Klamath

Mountains Province in the south and the Siletz Terrane in the north. The Klamath Mountains Province is a complex amalgamation of tectonostratigraphic terranes that represent oceanic volcanic arc complexes, associated forearc basin and accretionary prism mélange, and ophiolitic basement rocks which accreted to North America during the late Paleozoic and Mesozoic eras (Irwin, 1977; 1981; Blake et al., 1985a). The Klamath Mountains Province is flanked by late Jurassic and Cretaceous metasedimentary rocks referred to as the Coastal Belt. The Coastal Belt is correlative and largely continuous with the accretionary terranes of the Franciscan Complex in northern California (e.g. Irwin, 1977; Blake et al., 1985b).

The Klamath Mountains Province is overlain along its eastern and southeastern margins by Late Cretaceous shallow marine rocks (Hornbrook Formation and associated units) (Nilsen, 1984a; 1984b). These units are directly overlain by early Tertiary marine sandstones and conglomerates of the Payne Cliffs Formation (McKnight, 1984), which are in turn buried by Tertiary volcanics associated with the Cascade arc. Notably, the eastward-younging facies architecture of the Late Cretaceous Hornbrook Formation records an extensive marine transgression that occurred from at least Hauterivian to Turonian time (Sliter et al., 1984). This implies that the present-day domal topography of the Klamath region must post-date the Late Cretaceous and early Tertiary (e.g., Mortimer and Coleman, 1984).

North of the Klamath Mountain Province, the Siletz Terrane is a tectonostratigraphic terrane comprised of thick oceanic crust that accreted to North America during the Eocene (Wells et al., 2000; Wells et al., 2014). Basement rocks of the Siletz River Volcanics (Wells et al., 2014) are exposed sporadically along the

northwestern margin of the Coastal Belt terranes, where they are buried by a thin sequence of sedimentary rocks (Umpqua Group, Wells et al., 2000) derived from North America. Both the Siletz basement and Umpqua Group cover sequence were deformed during accretion to North America, and subsequently buried beneath a 1-2 km-thick accumulation of Eocene – Miocene shelf-slope sedimentary sequences (Heller et al., 1985; 1987). Unlike the Klamath terranes, comprising tilted and thrust-bound slices of accretionary terranes, the Siletz Terrane in Oregon appears to be a relatively coherent block of thick, dense oceanic crust that extends to the base of the North American lithosphere (Trehu et al., 1994).

2.2 *Coast Range Topography and Geomorphology*

Along-strike variations in the topography of the Cascadia forearc have long been hypothesized to reflect differences in the long-term uplift of rock above the subduction zone (McNutt, 1983; Kelsey et al., 1994; VanLaningham et al., 2006). Mean elevations in the central Oregon Coast Ranges range from ~200-300 m above sea level, and topographic relief typically ranges from 100-200 m (Figure 2). South of ~43°N latitude, however, mean elevations increase to ~1000 m above sea level, and topographic relief increases to ~800 m (Figure 2). As noted above, this broad increase in topography coincides with an abrupt step in the geodetic uplift rates from ~1 mm/yr to ~4 mm/yr (Figure 1c), typically interpreted as reflecting the position of the coastline relative to the locked Cascadia subduction zone interface (Burgette et al., 2009).

Long-term rates of rock uplift along this transect are known from marine terraces along the coast (e.g., Kelsey, 1990; McInelly and Kelsey, 1990; Kelsey and Bockheim,

1994) and inferred from the rates of fluvial incision (Personius, 1995) and/or erosion (Balco et al., 2013; O'Connor et al., 2014) from watersheds that drain the coast ranges. Although the rates of rock uplift inferred from marine terraces along the coastline exhibit short-wavelength variations associated with deformation along active upper-plate faults (e.g., Kelsey et al., 1996), the average rate of rock uplift relative to mean sea level along the central Oregon coast (north of latitudes ~43.5° N) is modest, ranging from 0.1 – 0.2 mm/yr (Kelsey et al., 1994; Van Laningham et al., 2006), with the exception of an elevation region near Newport, OR (~44.5°N; Kelsey et al., 1996). South of 43.5° N, however, the average uplift rates increase to ~0.5 mm/yr, with rates reaching ~1 mm/yr near active faults (Kelsey et al., 1994; Simms et al., 2015). These data suggest the possibility of a broad association between the high topography in the southern Cascadia forearc and long-term uplift rates.

Erosion rates from watersheds draining the Coast Ranges exhibit a similar increase from central to southern Oregon. Exploiting a data set of sediment accumulation behind historic reservoirs, O'Connor et al. (2014) developed estimates of sediment yield from rivers draining both the Coast Ranges and western Cascades. Comparison of the Rogue River, which drains the high topography of the Klamath region, with the Umpqua River, which drains lower relief regions of the Oregon Coast range underlain by the Siletz terrane, suggests that the Rogue watershed carries nearly twice the bedload flux of sediment (O'Connor et al., 2014). Although this was interpreted to reflect differences in the resistance of substrate lithology to erosion, it may also reflect differences in the long-term differential uplift of rock across these regions.

Recent analyses of watershed-average erosion rates using concentrations of the cosmogenic isotope ^{10}Be support the interpretation that long-term erosion rates are higher in the southern Cascadia forearc. Balco et al. (2013) collected a suite of samples from coastal watersheds along the Oregon and northern California Coast ranges (Figure 1). Erosion rates in central Oregon range from ~100-150 m/Myr, consistent with both fluvial incision rates (Personius, 1995) and with measures of hillslope erosion rate in this region (e.g., Reneau and Dietrich, 1990; 1991; Heimsath et al., 2001). However, erosion rates measured from watersheds in southern Oregon and northern California are up to 2-3 greater (Balco et al., 2013).

The hypothesis that variations in the topographic form of the Oregon Coast Ranges reflects spatial differences in rock uplift and/or erosion rate has been tested to some degree by evaluating the geomorphology of fluvial systems. In an effort to evaluate the controls on the shape of channel longitudinal profiles, VanLaningham et al. (2006) evaluated a set of trunk channels in select watersheds. This work showed that, while the concavity of the channels varied strongly with lithology, differences in channel steepness were modulated by both local differences in substrate erodibility and regional trends in rock uplift rate (VanLaningham et al., 2006). A similar study, restricted to monolithologic basins in the central Oregon Coast Range, found that steeper channels were localized above folds within the range and suggested that differential rock uplift was likely sustained along the core of the range (Kobor and Roering, 2004).

Collectively, the association of high topography, high rates of modern (geodetic) uplift, and elevated rates of rock uplift along the coast suggest the possibility that topographic relief in the Klamath province reflects ongoing deformation of the North

American plate inboard of the Gorda slab (e.g. McNutt, 1983) and north of the Mendocino Triple Junction (e.g., Wells et al., 1998; Wells and Simpson, 2001). However, there have been no detailed assessments of the tectonic geomorphology of the watersheds in the southern Cascadia forearc. Here, I focus on the Rogue River and adjacent watersheds. To evaluate the degree to which variations in topographic form may reflect spatial differences in differential rock uplift both along strike of the forearc and across strike, I evaluate the patterns of channel steepness (e.g., Kirby and Whipple, 2012) and compare these to a known data set that relates channel steepness to erosion rate (Balco et al., 2013).

3.   FIELD SITE: THE ROGUE RIVER WATERSHED

The Rogue River watershed extends across the southern Cascadia forearc region from the Cascade Mountains to the Pacific Ocean (Figure 2). Although topography throughout the Rogue River watershed is broadly characterized by reasonably high mean elevations and topographic relief, relative to the central Oregon Coast Ranges farther north (Figure 1), there are important differences in both elevation (Figure 2) and topographic relief (Figure 3) between the eastern headwaters and the western reaches of the river system. The coastal, western region of the watershed is characterized by peak elevations that reach ~1200 - 1500 m (Figure 2) and topographic relief of up to 1000 m between peaks and adjacent valleys (Figure 3). In contrast, the central portion of the watershed is characterized by peaks of similar elevation, but lower relief (Figure 3).

These differences are reflected in the geomorphology of the river valleys. The western watershed is characterized by the deeply incised canyons along the Rogue and

Illinois Rivers, where they are designated part of the National Wild and Scenic Rivers System. The central watershed, however, is characterized by broad, low-relief valleys filled with alluvial deposits (Figure 3). The boundary between these two domains is sharp and coincides with a NNE-trending mountain front that extends from approximately the OR-CA border southwest of the town of Cave Junction to northwest of Grants Pass (Figure 2) and is coincident with a series of high-angle faults, herein referred to as the "Eight-Dollar Fault", for a local peak that is located near the midpoint of the mapped structure (Figure 3).

Notably, these differences in landscape morphology are not directly coincident with terrane or lithologic boundaries. From its headwaters in the Cascade Range, the Rogue River flows primarily across terranes of the Klamath Mountains Province, just south of the boundary between the Klamaths and the Siletz Terrane (Figure 4). The headwaters of the Rogue River drains Oligocene – Recent volcanic rocks related to constructional volcanism of Cascade arc at elevations > 2000m, topographic relief in this region primarily reflects volcanic edifices. The central reaches of the river system drain a series of terranes including the May Creek, Rattlesnake Creek, and Western Hayfork (Snoke and Barnes, 2006). The western reaches of the river system, including the primary tributary of the Illinois River, drain across the Western Klamath Terrane and the Coastal Belt (Figure 4). The Eight Dollar Fault and the abrupt change in landscape morphology associated with it occur within the Western Klamath Terrane (Figure 4). The linear trace of the fault and the juxtaposition of intrusive igneous rocks against depositional marine metasedimentary rocks on the east of the structure suggest that it is likely a high angle reverse fault (Irwin, 1994; Yule, 1996; Figure 4; Figure 5). Although it is near the

boundary between the Western Klamath Terrane and the more easterly terranes (Figure 4, 5), it does not appear to have been one of the primary thrust systems across which these tectonostratigraphic blocks were juxtaposed (e.g., Snoke and Barnes, 2006).

The spatial transition from broad, alluviated valleys to high relief, confined channels also appears to mark a change in the geomorphic character of fluvial systems along the trunk channels of the Rogue watershed. East of the Eight Dollar Fault, the mainstem of the Rogue and the Illinois River are bounded by alluviated floodplains into which are notched a series of cut-in-fill terraces (Figure 6). Along the Rogue River, the mantle of alluvium is relatively thin, and bedrock outcrops along the banks (Figure 7). However, along the Illinois River, the alluvial fill reaches a thickness > 180 meters. Relief in the sub-alluvial bedrock must be substantial, however, as bedrock outcrops intermittently along the banks of the Illinois River.

In contrast, the Rogue and Illinois rivers west of the fault become confined by steep canyon walls decorated with narrow, discontinuous strath terraces (Figure 7). These strath surfaces are generally present along the trunks of the Rogue and Illinois Rivers, but are not evident along many side channels or tributaries. Terraces are capped by thin alluvial deposits consisting of coarse cobbles and boulders. These differences in the character of the river systems suggests that the differences in landscape relief on either side of the Eight Dollar Fault are associated with differences in the relatively recent incisional history of the fluvial systems.

The high topography in the western portions of the watershed generates a modest orographic rain shadow. The pattern of precipitation broadly mimics mean elevation, where the high elevation coastal ranges receive significantly more precipitation (3-5 m)

than the lower elevation valleys upstream (1-2 m) (Figure 8, PRISM Climate Group). A steep gradient in these observations coincides with the boundary between high relief and low relief regions across the 8 Dollar Fault. Precipitation increases again, locally and over more restricted areas, in the High Cascades region.

To evaluate the hypothesis that the differences in landscape morphology across the Eight Dollar Fault are associated with differences in rock uplift, I have conducted detailed stream profile analysis of major channels and their tributaries across the Rogue River watershed. I exploit a pre-existing, regional data set of long-term erosion rate (Table 1; Balco et al., 2013) that includes the Rogue watershed to develop a local scaling relationship between channel steepness and erosion rate (e.g., Kirby and Whipple, 2012). Together, these approaches allow investigation of the range of possible variations in erosion rate across the Rogue watershed and allow me to evaluate drivers for spatial patterns in channel morphology and incision.

4.   METHODS

4.1   Stream Profile Analysis

The recognition of the dynamic interplay between climate, surface processes, and the geodynamics of orogenic belts led to an explosion in the study of tectonic geomorphology (Molnar and England, 1990; Raymo and Ruddiman, 1992). Much of our current understanding of the way in which climate and erosion are coupled relies on the processes that set the shape of actively incising river profiles and topographic relief (e.g. Whipple et al., 1999). In regions of uniform rock strength, climate, and rock uplift rate, steeper channels should be associated with higher erosion rates and, at steady-state

(Willett and Brandon, 2002), higher rates of rock uplift (Whipple et al., 1999). The longitudinal profiles of bedrock rivers in mountainous terrain have long been recognized to demonstrate a power-law type scaling relationship between channel slope (S) and contributing drainage area (A) of the following general form (Hack, 1957; Flint, 1974):

$$S = k_s A^{-\theta} \tag{1}$$

where the pre-exponential constant, k_s, is a measure of channel steepness and θ is an index of channel concavity (the rate of change of gradient with increasing drainage area). To compare channel steepness among different channel segments, one must account for correlations between the concavity and steepness indices (e.g., Kirby et al., 2003; Wobus et al., 2006), accomplished by using a fixed reference value for the concavity index ($\theta_{ref} = 0.45$) that yields a normalized channel steepness index, k_{sn} (Snyder et al., 2000; Kirby and Whipple, 2001; Duvall et al., 2004):

$$S = k_{sn} A^{-\theta_{ref}} \tag{2}$$

The boundary between channel reaches of different steepness can be determined by regression of channel gradient versus drainage area in log-log space (see Wobus et al., 2006; Kirby and Whipple, 2012 for a detailed explanation of methods).

Channel steepness of stream profiles can also be evaluated as the scaling of a parameter chi (χ) with elevation in the catchment (Harkins et al., 2007; Royden and Perron, 2013). Chi represents the integral of contributing drainage area (A) with respect to streamwise distance (x) (e.g. Perron and Royden, 2013) as:

$$\chi = \int_{x_b}^{x} \left(\frac{A_0}{A(x)} \right)^{\theta_{ref}} dx \tag{3}$$

where x_b is the position at the river mouth and A_0 is a reference drainage area. When A_0 is set to 1 km^2 and θ_{ref} to the same value as used in equation (2), the slope of the chi-

elevation plot is equivalent to the normalized steepness index (Royden and Perron, 2013).

For a simple equilibrium profile, this transformation yields a line of uniform slope (k_{sn})

when plotting chi (χ) vs. elevation (z). Chi has proven useful in evaluating equilibrium

conditions along single stream profiles and in comparing stream profiles as it allows

comparison of streams with different drainage areas while eliminating discontinuities

resulting from abrupt increases in drainage area at tributary junctions (Perron and

Royden, 2013; Willett et al., 2014). Profiles that exhibit a change in slope along the

profile indicate a spatial variation in the equilibrium conditions along the channel. Stream

profiles that diverge in chi-space are interpreted to be adjusted to different equilibrium

conditions.

It is important to note that these scaling relationships along channels only hold

above some critical contributing area (A_{cr}), generally $A_{cr} > 1$ km^2 (e.g. Montgomery and

Foufoula-Georgiou, 1993), that represents a transition to hillslope processes above the

channel head (e.g., Kirby and Whipple, 2012). Although there is a potential influence of

debris-flows processes on the position of this scaling break (Stock and Dieterich, 2003),

the analysis presented here evaluates channel steepness as a function of streamwise

position up to 1 km^2.

These methods of interpreting stream profile steepness also allow recognition of

knickpoints as distinct changes in the scaling of gradient with drainage area (Wobus et

al., 2006; Kirby and Whipple, 2012; Perron and Royden, 2013). We follow Kirby and

Whipple (2012) in identifying two morphologic types of knickpoints; slope-break

knickpoints are associated with a distinct change in channel steepness among two or

more reaches of channel, whereas vertical-step knickpoints are isolated, steep reaches of

channel across which there is no change in k_{sn} (see Kirby and Whipple, 2012). The former have the potential to represent migrating boundaries in the landscape between a relict portion of the fluvial network that has not yet been affected by a transient wave of incision (e.g., Crosby and Whipple, 2006; Kirby and Whipple, 2012).

4.2   Extraction and interpretation of river profiles

Digital elevation data sets (DEM) used in all analyses was prepared and channels were extracted according to the methods of Wobus et al. (2006). I used data from the National Elevation Dataset (NED) with nominal resolution of 30m. To smooth raw elevation data along river channels, I applied a moving average smoothing window of 1 km (Kirby and Whipple, 2012). Channels were extracted downstream from channel heads and normalized channel steepness was calculated using a reference concavity (θ_{ref}) of 0.45 to enable comparison with published datasets.

4.3   Scaling between channel steepness and erosion rate

Datasets from mountain belts across the globe reveal distinct scaling relationships between k_{sn} and basin-wide, long-term erosion rates (E) where increasing erosion rate generally corresponds to increases in rock uplift rate (Kirby and Whipple, 2012). Differences among field sites are thought to reflect differences in rock mass quality that govern the erodibility of rock (e.g., Forte et al., 2016) and/or the influence of climatically modulated discharge regimes (Lague et al., 2005; DiBiase and Whipple, 2011) that govern the effectiveness of fluvial erosion. Regardless, in a given climatic setting, these

data suggest the possibility that variations in channel steepness (k_{sn}) may allow assessment of the spatial patterns in erosion rate across a mountain range.

In this study, I exploit an existing cosmogenic erosion rate dataset to develop a regional scaling of erosion rate and channel steepness in the Oregon and northern California Coast Ranges. I determined the basin-wide average channel steepness (k_{sn}) for basins throughout the forearc where basin-average erosion rates were independently measured using cosmogenic isotope concentrations in modern sediment (Balco et al., 2013). The existing cosmogenic erosion rate dataset includes watersheds that drain the Oregon and northern California coast ranges to the Pacific Ocean, including the Rogue River (Figure 1; Balco et al., 2013). This dataset exhibits a positive correlation between the basin-wide averaged channel steepness (k_{sn}) and measured cosmogenic erosion rate of the contributing catchments (Balco et al., 2013). Due to the latitudinal range covered by the dataset, it incorporates broadly representative variations in climate, bed lithology, and crustal structure, yet demonstrates a strongly positive correlation with uplift rate. These relationships suggest that spatial variations in channel steepness (k_{sn}) in the region should provide at least a qualitative assessment of spatial variations in erosion rate.

Basin averaged channel steepnesses (k_{sn}) were calculated for the areas upstream of sampling locations in Balco et al. (2013). Because this dataset includes watersheds draining the coastal ranges of the Cascadia forearc from the Columbia River gorge to northern California near Cape Mendocino, it incorporates a range of lithologies. Watershed boundaries were delineated and extracted from 30m NED data upstream of locations sampled by Balco et al. (2013). A channel network was extracted from each watershed's bounds following the procedures of Wobus et al. (2006). Channels with a

minimum contributing drainage area of 1 km^2 were included in the steepness calculation.

Channel smoothing was conducted over a 250 m moving average. From the resulting

network, channel steepness was calculated for channel segments of 1 km length, and then

averaged to produce a value for the entire drainage basin (e.g., Ouimet et al., 2009).

To create a spatially continuous map of channel steepness, I conducted a spatial

interpolation of k_{sn} values along the channel network in the Rogue watershed using a 5

km circular moving average (Kirby and Ouimet, 2011). I fit a power law regression to

the channel steepness and erosion rate of Balco et al. (2013) (Table 1). The Rogue River

watershed falls well within the bounds of the dataset with respect to geographic location,

basin averaged erosion rate, and basin-wide channel steepness (Balco et al., 2013). This

power law relationship was then used to develop an estimate of long term erosion rate

across the Rogue River watershed. The resulting raster was averaged using a 5 km

circular moving window to generate a spatially averaged map of long term erosion rates.

5   Results

5.1   Channel Steepness

The pattern of channel steepness across the Rogue River watershed broadly

corresponds to landscape morphology and relief across the watershed. Channel steepness

values in the Cascade Arc are high; both the greatest local relief (~915 m) and channel

steepness (>250 m$^{0.9}$) correspond with the incised canyons through which the Rogue and

its tributaries flow out of the Cascade Arc into the Klamath Mountains Province. In

contrast, across the center of the watershed, where the Rogue River flows across

lithologies of the Klamath Mountains Province and its comprising terrains, lower order

channels are generally steep. Where lower order channels reach low relief valleys,

channel gradients and channel steepnesses (k_{sn}) decrease precipitously. Here, lower order

channels are primarily consolidating with one of two trunk channels, the Rogue River and

the Illinois River.

To the west of the Eight Dollar Fault, the Rogue watershed is characterized by

steep channels. The boundary between low gradient and high gradient channels occurs

most dramatically where the Rogue and Illinois truck channels cross the Eight Dollar

Fault. For channels with contributing areas greater than 1km^2, values of channel

steepness (k_{sn}) roughly double (from ~50 to ~100 m$^{0.9}$) across the Eight Dollar Fault

(Figure 9; Figure 10). The broad valleys associated with the Rogue and Illinois rivers

terminate where the channels cross the lineament corresponding with the location of the

Eight Dollar Fault. This change occurs over a streamwise distance of only a few

kilometers.

The regional differences in channel steepness are expressed in the longitudinal

profiles of the two trunk channels, the Rogue River and the Illinois River, where they

cross the Eight Dollar Fault. Both display a distinct increase in gradient and channel

steepness (k_{sn}) where they cross the Eight Dollar Fault (Figure 11). This increase in

gradient and channel steepness appears as a broad knickzone, a convex portion of the

river profile that deviates from the concave-up geometry expected of channels adjusted to

an equilibrium condition. The initiation of this knickzone occurs at an elevation of

~230m and ~375m on the Rogue and Illinois rivers respectively (Figure 11). Although

the knickpoints on the two channels occur at significantly different drainage areas (Rogue

$= 13,292$ km^2; Illinois $= 2,546$ km^2), they correspond to the transition from alluviated to incising rivers.

5.2   Stream Profile and Knickpoint Analysis

Tributaries to the Rogue and Illinois channels host numerous knickpoints, distributed throughout the watershed. Plotting knickpoints along the stream profiles, many knickpoints on the tributaries downstream of the Eight Dollar Fault occur at higher elevations than profile convexities along the Rogue or Illinois trunk channels (Figure 12; Figure 13). Two regions appear as stair steps along the longitudinal profiles, these lie on reservoirs and so have been removed from the knickpoint dataset (Figure 12; Figure 13). Knickpoints in the Cascade Arc region of the Rogue watershed are numerous and large. The largest of these correspond in map view to canyons cut into the thick volcanic apron along the boundary between the Cascades and Klamath Mountains.

In map view, knickpoints do not appear to be distributed across the watershed systematically (Figure 14). Some channels host more than one knickpoint, whereas others do not host any, and knickpoints are distributed throughout the large watershed across a wide range of elevations (Figure 12). A minority of the knickpoints identified lie on lithologic contacts (Figure 14). It is worth noting that where those knickpoints are associated with lithologic contacts, they are also associated with longer bedrock faults.

5.3   Calibrated Erosion Rate

Based on the globally observed scaling relations between k_{sn} and basin-wide erosion rate (Kirby and Whipple, 2012), I make use of an existing cosmogenic erosion rate dataset for

watersheds draining the Oregon and northern California coast ranges into the Pacific Ocean (Table 1; Figure 15; Balco et al., 2013). This dataset demonstrates a power-law scaling relationship between basin-wide erosion rates and watershed averaged channel steepness (k_{sn}) in concert with a correlation to uplift gradients along the Cascadia forearc. Further, this dataset incorporates variations in lithology both along and across the forearc including the domains of Siletzia, the Klamath Mountains Province, and the Franciscan Assemblages of the California coastal belt.

The interpolated map of erosion rates across the Rogue watershed reveals a clear variation in erosion rate across the Eight Dollar Fault (Figure 16). The region of high k_{sn} west of the fault is associated with an average predicted erosion rate of 0.75 mm/yr and reaches maximum values of ~1.5 mm/yr maximum. In contrast, predicted erosion rates east of the fault average 0.3 mm/yr average and reach a maximum value of ~0.9 mm/yr. Areas of steep channels in the headwaters, near the watershed divide, and where channels drain the high Cascades also predict relatively high erosion rates based on the calibration.

6 Discussion

Along the Cascadia subduction zone forearc, an increase in mean elevation and relief from north to south is consistent with the structural boundary between the Siletz Terrane and the accreted Klamath Terranes (Figure 1). However, the co-variation between short-term and geological timescale observations and proxies for uplift suggest that there is dynamic support and contribution to the modern signature of long wavelength, regional topography. Dynamic drivers such as subduction zone driven block rotation (Wells, 1998), heterogeneity in the age and roughness of the downgoing slab

between the Juan de Fuca and Gorda plates (McNutt, 1983), northward migration of the Mendocino Triple Junction, and convergence of the Sierra Nevada block are all potential geodynamic mechanisms that could drive uplift and deformation in the southern Cascadia forearc (Furlong & Govers, 1999).

Although in principle, these geodynamic mechanisms may be differentiated based on the patterns of channel steepness (k_{sn}) and knickpoint distributions that would result from various space-time patterns of differential rock uplift, here I focus on potential explanations for variations in channel steepness (and predicted erosion rate [Figure 16]) across the Eight Dollar Fault. I compare observations of channel steepness and knickpoint position to simple expectations for differential rock uplift localized along the fault, transient incision in response to a recent fall in relative base level, lithologic resistance to erosion, and the effect of orographic variations in precipitation and runoff.

Differential uplift of a downstream block would result in channel incision downstream and aggradation upstream of the accommodating fault. Furthermore, knickpoints generated under this scenario should remain stationary, anchored along the trace of the fault. Finally, a significant drop in base level would result in a wave of knickpoints migrating throughout the channels and tributaries of the watershed.

6.1   Orographic precipitation

It is relatively well-known that climatically induced changes in effective discharge strongly modulate the steepness of river profiles (Whipple and Tucker, 2002; Snyder et al., 2003; DiBiase and Whipple, 2011). In general, for a given rate of differential rock uplift and similar lithologic substrate, we expect regions of greater

precipitation and runoff to have lower equilibrium channel steepness. In the study area, the highest channel steepnesses (k_{sn}) are found in the western part of the watershed, and are coincident with the region of greatest precipitation (Figure 8). This is the opposite distribution of channel steepness and gradients that would be expected given the observed pattern of long-term precipitation. Thus, the differences in channel steepness and landscape relief do not simply reflect orographic precipitation. If anything, they suggest that steep channels are maintained in the lower portions of the Rogue and Illinois watershed despite higher precipitation and runoff.

6.2   Transient Incision Related to Base-Level Fall

One possible explanation for the steeper channels in the western part of the study area is that they represent a transient response to a recent increase in uplift rate in the Cascadia forearc. In the simplest case, knickpoints generated in such a system represent a transition between downstream reaches of the fluvial network which are steepened and adjusted to the new rate of rock uplift from upstream reaches that are still adjusted to the former condition (e.g., Whipple, 2001). Most models for bedrock river incision characterize this response as a kinematic wave (Rosenbloom and Anderson, 1994), where the speed of the knickpoint depends on discharge/drainage area (Crosby and Whipple, 2006; Harkins et al., 2007). Notably, these knickpoints migrate up the channel network at a constant vertical velocity (Niemann et al., 2001) such that their spatial distribution at a given time should be approximately equal elevation (e.g., Wobus et al., 2006).

We restrict our consideration to knickpoints downstream of the Eight Dollar Fault. Knickpoints upstream of the broad knickzones on the Rogue and Illinois trunk

channels must be, by their position, either be related local spatial heterogeneities (locally-resistant rocks or faults) or to local volcanic activity (tephra accumulation associated with the Mazama eruption, for instance). If knickpoints east of the Eight Dollar Fault represent a transient response to base level fall, they would have had to pass through the convexities along the Rogue and Illinois trunk streams and thus likely do not hold insight to the nature of these knickzones on the Rogue and Illinois trunk channels.

In the region west of the fault, knickpoints are not systematically distributed throughout the fluvial network in either elevation or drainage area (Figure 12). Athough there is an apparent cluster of knickpoints at ~700-800 m elevation (Figure 12), these are significantly higher elevation than the knickzones on the Rogue and Illinois trunk channels (Figure 11). Thus, they are not easily explained as a migrating wave of channel adjustment (Niemann et al, 2001) that is linked to the knickzones on the Rogue and Illinois rivers.

Finally, the position of knickzones along the Rogue and Illinois trunk streams are themselves not easily explained by a kinematic wave model (Niemann et al., 2001). The kinematic wave model for knickpoint propagation suggests that, under uniform conditions, channel adjustment to uplift is functionally related to channel gradient and drainage area such that streams of lower drainage area adjust to a higher gradient (Niemann et al., 2001). This results in a systematic wave of channel adjustment that leads to clusters in elevation space. Notably, the position of knickzones on the Illinois and Rogue channels sit at different elevations (230 m versus 375 m, Figure 11), at very different drainage areas (Rogue = 13,292 km^2; Illinois = 2,546 km^2), both of which are inconsistent with these features having been generated in response to a single transient

response. Rather, their coincidence with the location of the Eight Dollar Fault strongly suggests a genetic association with this structure.

6.3   Lithologic Resistance to Erosion

Knickpoints across the watershed are not systematically located along mapped lithologic boundaries (Figure 14). The distribution of knickpoints throughout the Rogue watershed suggests that lithology is playing a secondary role in topographic expression across the Klamath Mountains Province (Figure 14). Previous authors have noted that knickpoints are just one manifestation of lithologic control across the Cascadia forearc, others include sediment flux variations, grain-size variation, and landslide occurrence (VanLaningham et al., 2006; Kobor and Roering, 2004; O'Connor et al., 2014). Variation in mean elevation and relief across the Rogue watershed does not generally correspond to lithologic variation except along the margin of the Cascades Arc and across the 8 Dollar Fault. The inconsistent occurrence of knickpoints at lithologic contacts throughout the region further suggests that lithology is a second, or even third order control on local landscape expression across the Klamath Mountains Province**.**

6.4   Differential Rock Uplift

The simplest explanation for the spatial differences in topographic relief and mean channel steepness across the Eight Dollar Fault is that this structure accommodates differential uplift of the western part of the Cascadia forearc relative to the eastern forearc and arc. For rivers flowing into a region of increasing rock uplift rate, we expect two effects: 1) rivers within the actively uplifting block will begin to incise and steepen, while 2) reaches upstream of the block will begin to deposit sediment and aggrade (Humphrey

and Konrad, 2000) (Figure 17). This scenario qualitatively explains the difference in both channel steepness and topographic relief across the fault, as well as the geomorphic difference between recent incision in the downstream reaches and aggradation upstream of the fault. Moreover, this also provides an explanation for the spatial coincidence of knickzones along the trunk channels of the Rogue and Illinois rivers with the trace of the fault.

Although it would be tempting to claim that the two-fold difference in channel steepness (k_{sn}) observed in the channel network across the Eight Dollar Fault represents a two-fold difference in uplift rate, the non-linearity of scaling between channel steepness (Figure 10) and erosion rate (Figure 16) suggests that the difference is in fact greater. Calibration of channel steepness (k_{sn}) as a proxy for average erosion rates (Figure 16) suggests that the block west of the Eight Dollar Fault may be eroding at rates up to 1.5 mm/yr, while the eastern block appears to be eroding more slowly (0.3 – 0.5 mm/yr). The association of steep channels and high precipitation in this block present a compelling argument that the topography must be sustained by relatively high rates of rock uplift. Previous mapping along the Eight Dollar Fault suggests that is a steeply dipping reverse fault (Irwin, 1994; Yule, 1996). As such, a majority of dip-slip motion on the fault would contribute to rock uplift, with little attendant crustal shortening. If the main stems of the Rogue and Illinois rivers are in landscape equilibrium, it is possible that throw rates along the Eight Dollar Fault could be up to ~1 mm/yr. Regardless of the exact rates, it seems reasonable to conclude that the fault controls differential vertical motions across this portion of the Cascadia forearc.

7 CONCLUSIONS AND TECTONIC IMPLICATIONS

The combination of topographic and geomorphic analyses presented herein support the following conclusions:

(1) Systematic spatial differences in channel steepness (k_{sn}) and topographic relief within the Rogue River watershed reflect differential uplift of rock between the western and eastern portions of the Cascadia forearc.

(2) Broad knickzones along the Rogue and Illinois rivers are coincident with the trace of the Eight Dollar Fault, but are not found at similar elevation or drainage area. This suggests that these features of the river profiles are fixed in space and reflect differences in uplift rate across the fault.

(3) Calibration of a regional scaling relationship between channel steepness and erosion rate suggests that the doubling in average channel steepness (k_{sn}) across the fault may be associated with a 3 to 5-fold increase in erosion rate. These estimates are minima, as greater precipitation and runoff in the western block may enable those channels to erode more efficiently.

In summary, differences in relief, mean elevation, channel steepness, surficial geology, and the presence of broad knickzones on the Rogue and Illinois rivers correspond to the location of the Eight Dollar Fault. Given these observations, I conclude that these variations are the result of ongoing differential uplift localized on this reactivated structure in the southern Cascadia forearc. This conclusion suggests that upper plate deformation is contributing to, and may be sustaining, topography in the southern Cascadia forearc. This result does not implicate a single geodynamic driver. However, this result does allow us to conclude that topographic variation along the southern

Cascadia forearc is being sustained by modern dynamics of the plate boundary and is not solely an artifact of ancient mountain building events.
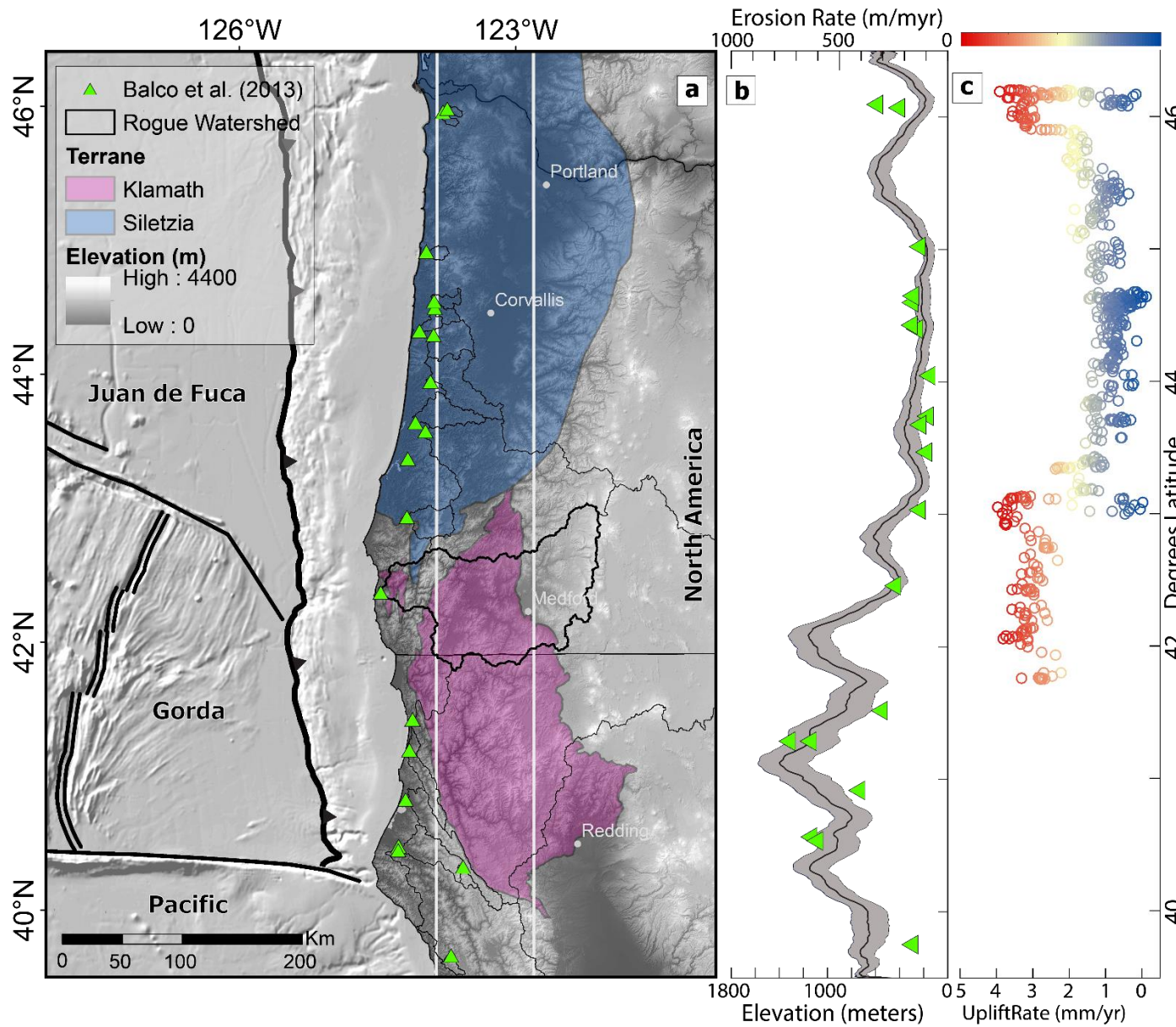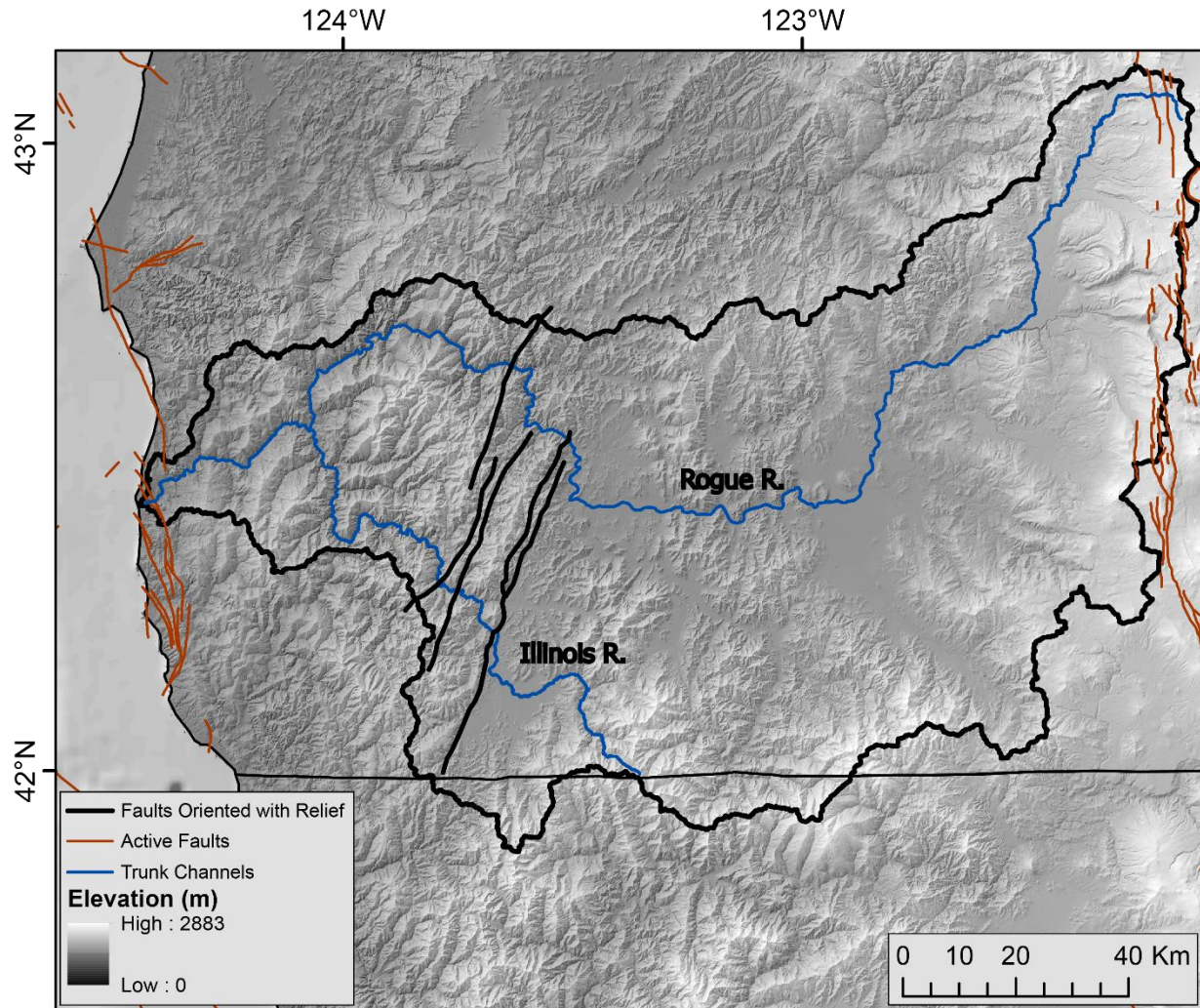
Figure 1.
(a) Grey to black colored elevation over hillshaded DEM above sea level, hillshaded bathymetry of the Pacific Ocean.
Thick black lines outline plate boundaries; teeth lie on the upper plate of the Cascadia megathrust. Doubled black lines
indicate the Chron 1A magnetic age contour (Wilson, 2002).
Green filled triangles are sample locations of Balco et al. (2013) averaged erosion rates.
Sinuous black outlines delineate sampled watersheds.
Silver bars bound the region from which swath topographic profile was calculated.

(b) Swath of topography from area bounded by silver bars in (a), smoothed using a 35 km moving average; upper and lower bounds indicate average minimum and maximum elevations, center line (black) follows average elevation. Green triangles plot watershed-averaged erosion rate (x-axis) for catchments from Balco et al. (2013).

(c) Geodetic uplift rates from Burgette et al. (2009). Geodetic uplift rate (mm/yr) increases to the left and corresponds to red-blue colormap.
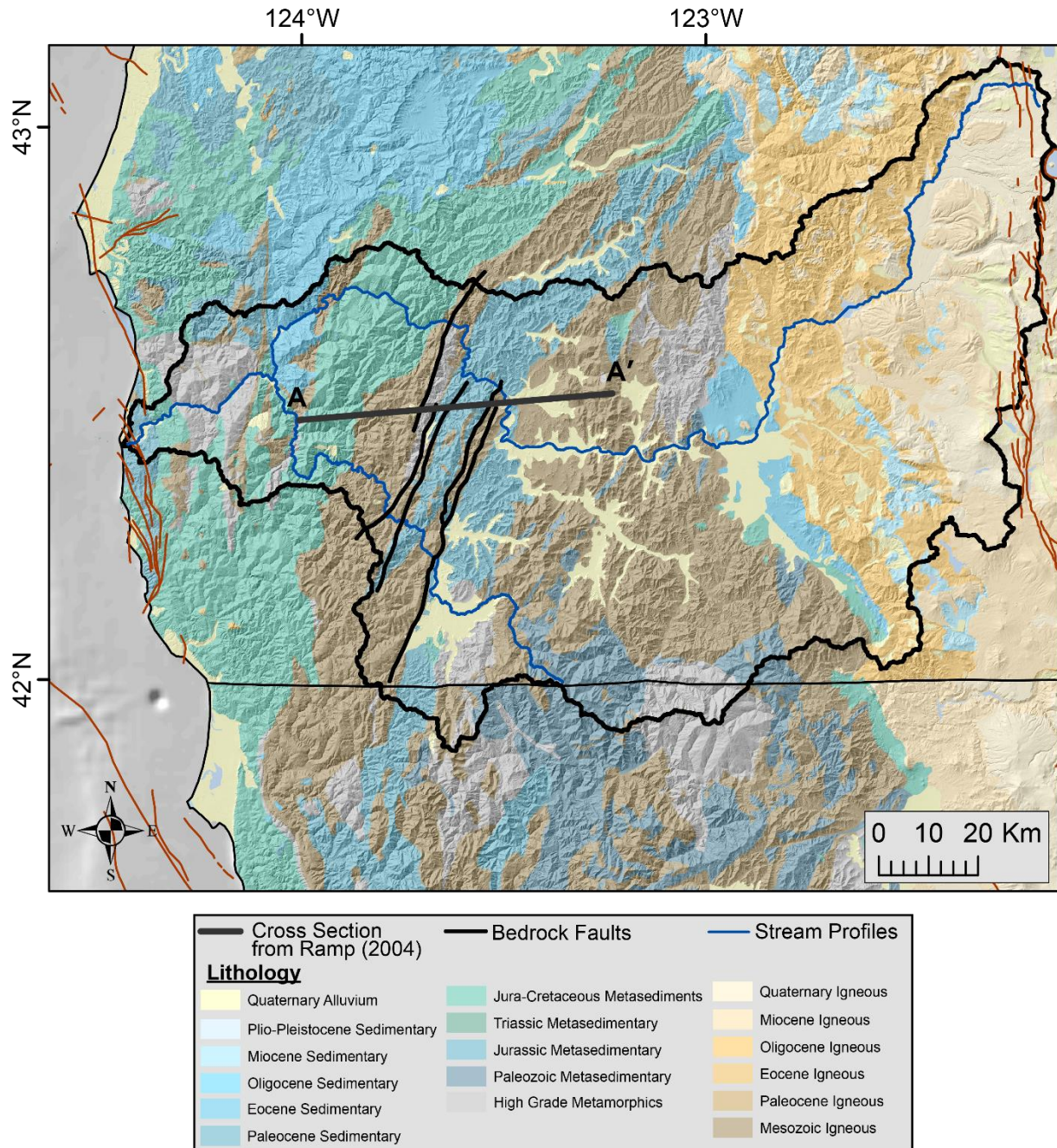
Figure 2.
Color-shaded DEM over hill-shaded DEM toporaphy for the Rogue River watershed. Red lines represent faults currently recognized as active per the USGS Quaternary Fault Database (2006). Black lines represent major structures located along or parallel to the boundary between low relief valleys and the high relief canyons downstream along the Rogue and Illinois rivers. Blue lines represent the trunk channels of the Rogue and Illinois rivers, Rogue watershed outline in heavy black.
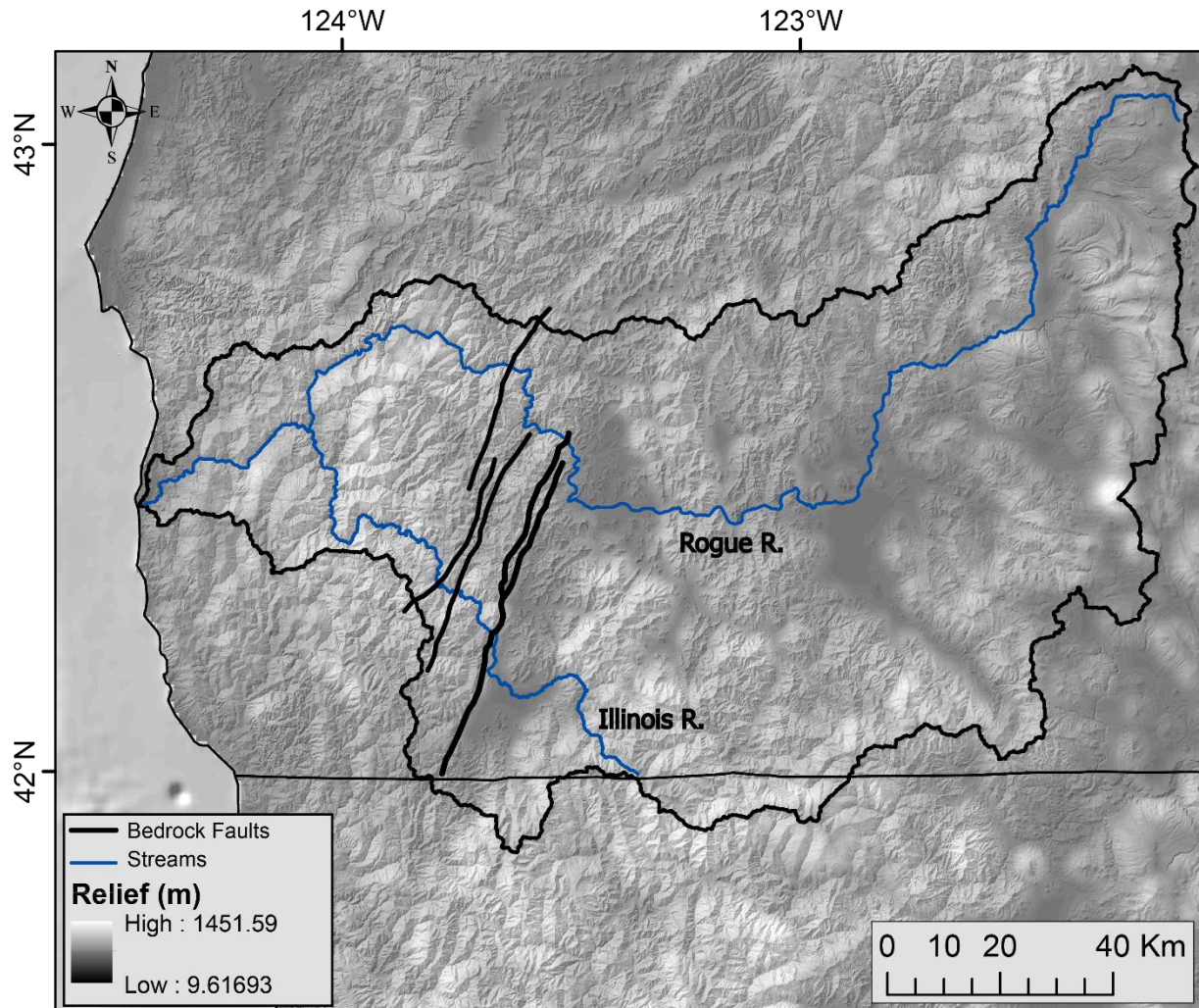
Figure 3.
Color shaded average relief over hillshaded DEM for the Rogue watershed; relief calculated using a circular radius of 1km and averaged using a circular moving window of 1km radius. Structures of interest represented by heavy black lines; trunk channels of the Rogue and Illinois rivers displayed as blue lines, the Rogue watershed is outlined in black.
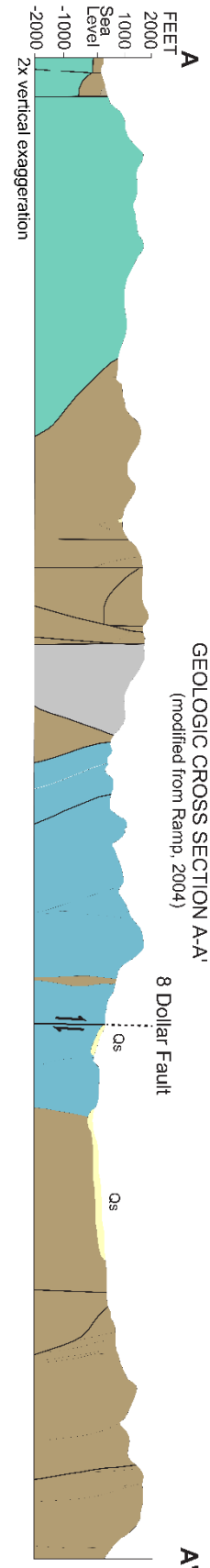
Figure 4.
General geology of the Rogue River watershed, organized by general age and rock type (OGDC-6, 2015). Thin red lines delineate active faults (USGS Quaternary Fault Database, 2006). Black lines represent faults oriented parallel to relief within the Rogue River watershed. Blue lines represent trunk channels of the Rogue and Illinois rivers, Rogue watershed outlined in black. The heavy gray line represents the cross section line of Ramp (2004).

Figure 5.
Schematic cross-section of line A – A' (Figure 4). Adapted from Ramp (2004), colors reflect general geology colored by age and general lithology (Figure 4).

Figure 6.
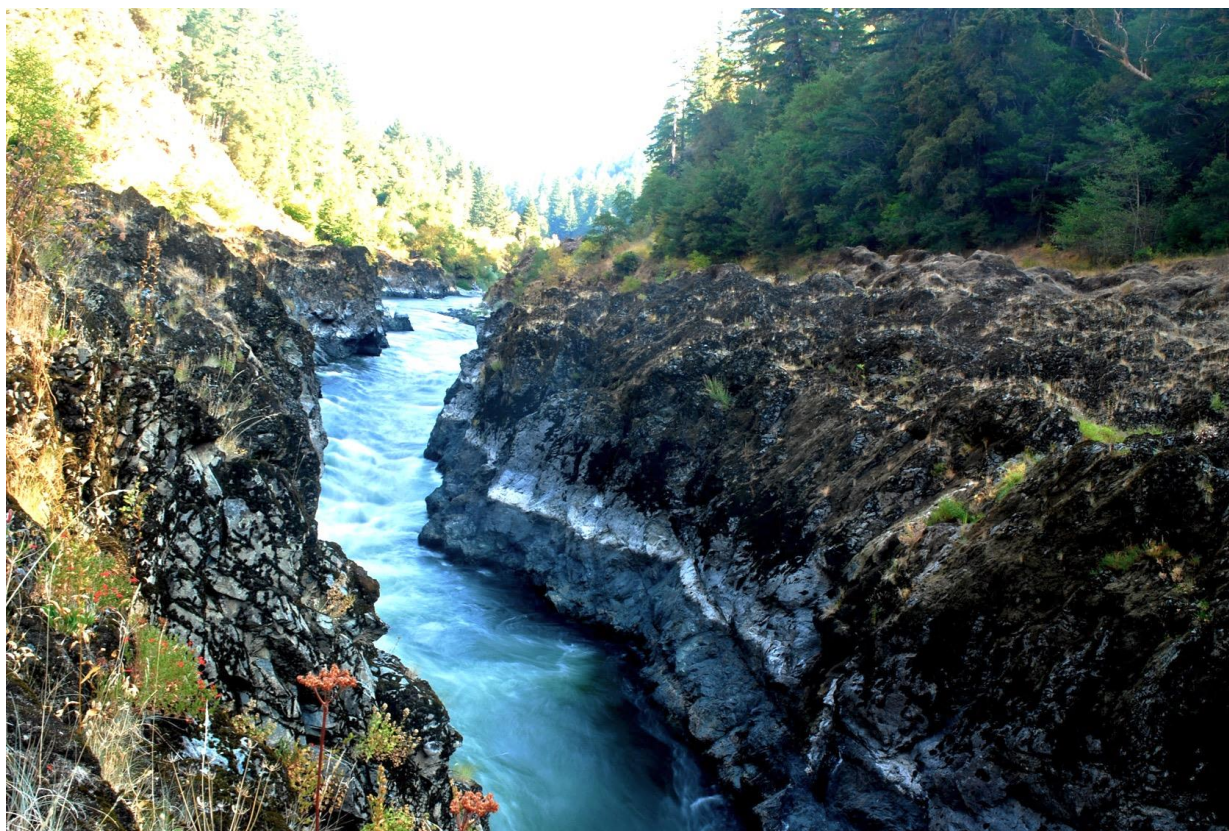An example of alluvial cut-in-fill terraces developed in the low relief valleys upstream of the 8 Dollar Fault. Here the terrace is ~8m tall. Relief corresponding to the 8 Dollar Fault is seen as the ridgeline in the upper left of the photo.

Figure 7.
Photo near Mule Creek Canyon, downstream of the 8 Dollar Fault, along the main stem of the Rogue River. The bedrock strath here is ~14m above the modern river level.
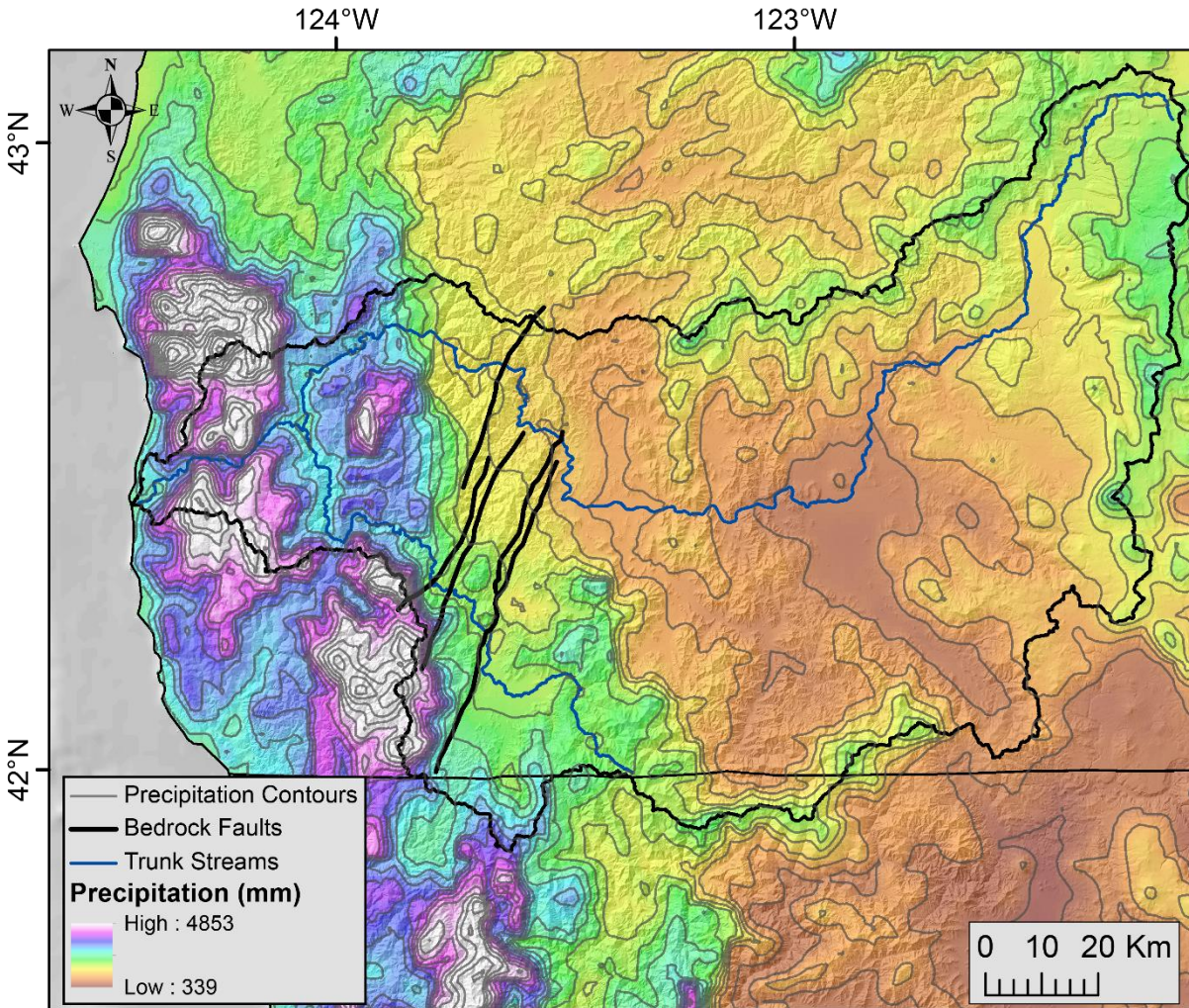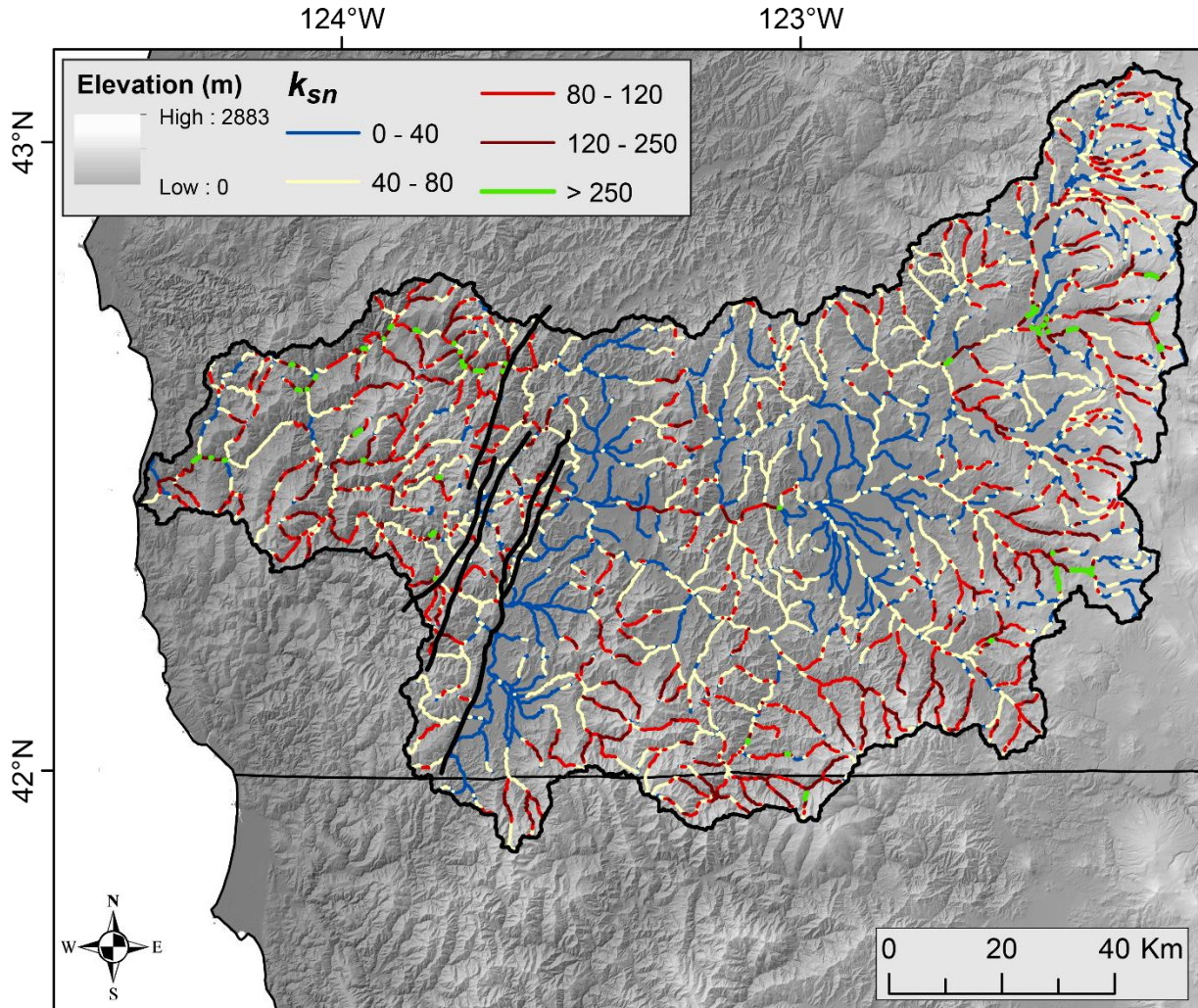
Figure 8.
Contoured precipitation data over hillshaded DEM. Contours spaced at 200mm interval, precipitation data are 30-year means (1981 – 2010; PRISM Climate Group). Black lines represent major structures aligned with relief in the Rogue watershed. Blue sinuous lines represent the trunk channels of the Rogue and Illinois rivers, black outline represents Rogue watershed boundaries.

Table 1.

Watershed Name	Watershed Averaged Channel Steepness Index [1]	Watershed Apparent Basin-scale Erosion Rate [2]	Watershed Area	Sample Location	
Watershed averaged channel steepness and apparent basin-scale erosion rates					
	(k_{sn})	(m Myr^{-1})	(km^2)	Latitude	Longitude
Eel River	90.03	643.5 ± 92.4	9265	50.568	-124.155
North Fork Klaskanine River	40.77	337.9 ± 25.7	69	46.094	-123.739
Youngs River	40.17	238.8 ± 19.1	88	46.070	-123.786
Salmon River	50.59	141.2 ± 11.8	155	45.023	-123.945
Yaquina River	25.36	173.2 ± 12	209	44.651	-123.857
Elk River	25.36	176.8 ± 12.3	220	44.603	-123.852
Drift Creek	32.54	180.71 ± 34.04	178	44.428	-124.005
Alsea River	34.0963	155.3 ± 11.4	895	44.399	-123.860
Siuslaw River	24.7	96.8 ± 7.2	1538	44.051	-123.886
Smith River	23.55	107.2 ± 8.4	910	43.743	-124.037
Umpqua River	64.24	138.7 ± 10.5	10893	43.678	-123.933
Sullivan Creek	48.48	111.22 ± 9.89	4	43.470	-124.113
Coquille River	63.04	141.8 ± 11.7	798	43.033	-124.114
Rogue River	**86.6**	**256.7 ± 21.8**	**13292**	**42.465**	**-124.369**
Redwood Creek	96.16	742.35 ± 56.48	714	41.289	-124.058
Mad River	94.59	422.4 ± 37.4	1265	40.917	-124.090
South Fork Eel River	90.88	616.5 ± 51.3	8150	40.535	-124.156
Van Duzen River	78.73	1109.8 ± 142.5	150	40.417	-123.518
Upper South Fork Eel Creek	35.89	177.73 ± 27.51	152	39.753	-123.629
North Fork Caspar Creek	16.25	182.44 ± 11.72	5	39.360	-123.735
South Fork Caspar Creek	23.87	124.21 ± 10.19	4	39.346	-123.755

[1] Calculated following general methods of Wobus and others (2006). See Appendix I for details.
[2] Data reported and apparent basin-scale erosion rates calculated and published by Balco et al. (2013).

Figure 9.

Channel network for Rogue watershed colored by binned channel steepness (k_{sn}) value. Channel steepness is mapped over color shaded elevation and hill-shaded topography. Black lines represent structures aligned with relief across the Rogue River watershed, black outline represents the boundary of the Rogue River watershed.
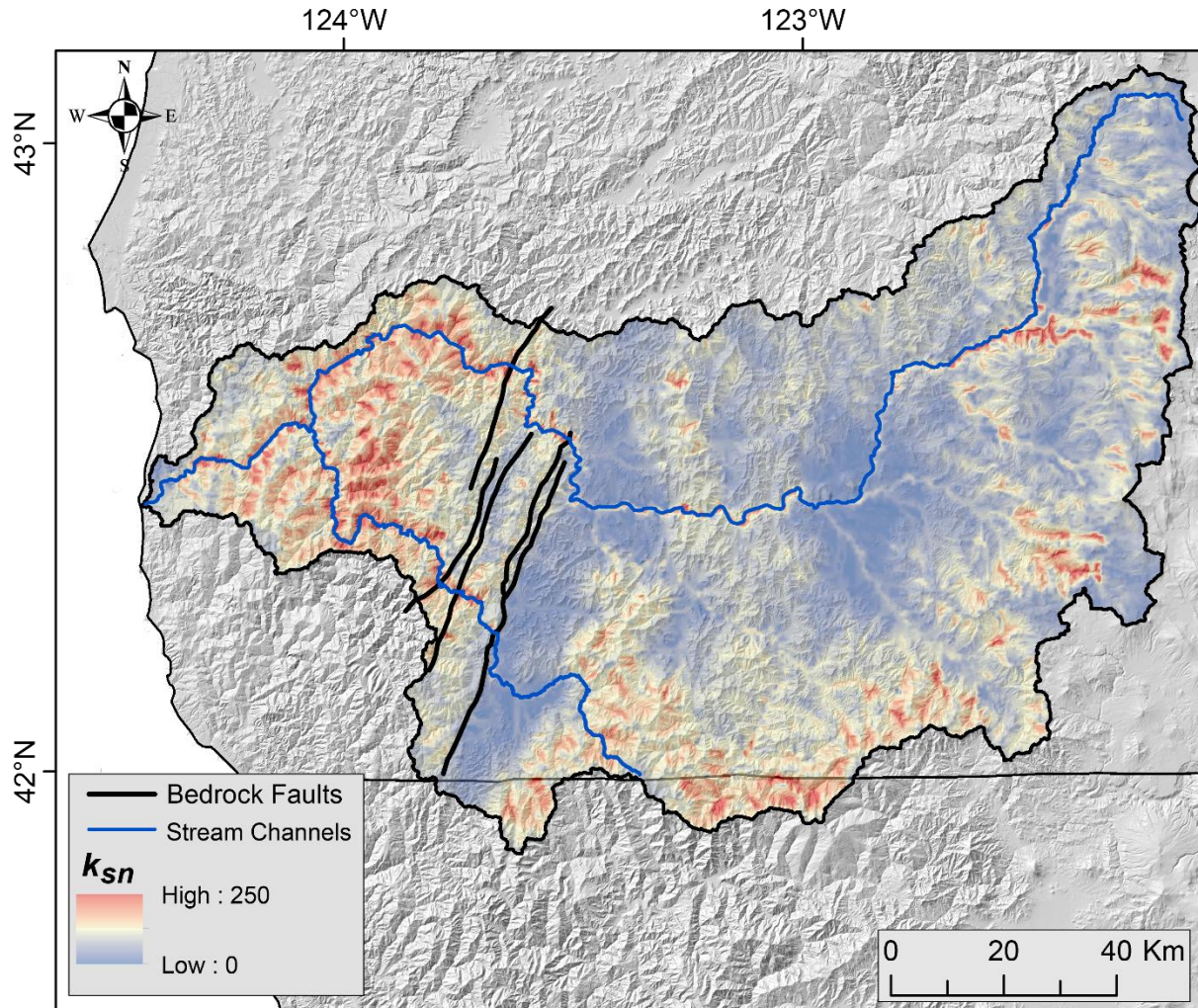
Figure 10.
Channel steepness (k_{sn}) raster interpolated from the channel network (Figure 9) within the Rogue River watershed.
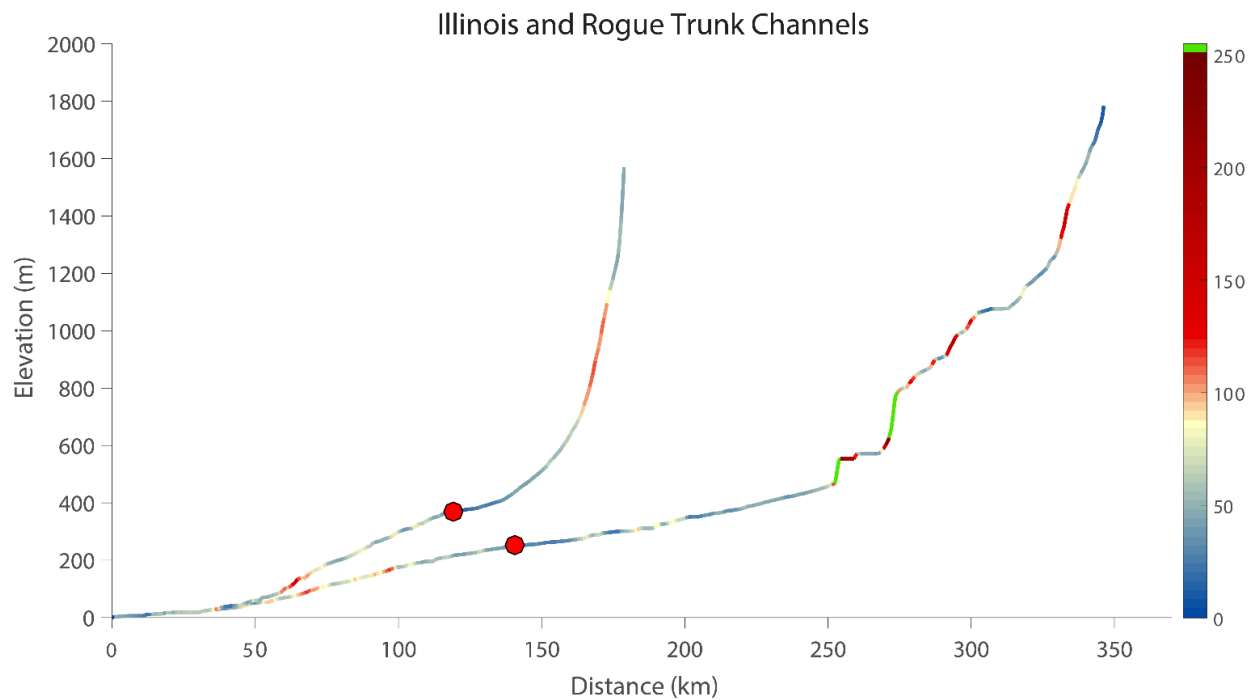
Figure 11.
Longitudinal profiles of the Rogue (right) and Illinois (left) rivers colored by channel steepness, k_{sn}. Large red circles are located where the 8 Dollar Fault intersects these channels in space, note the prominent convexity developed in each profile downstream of the 8 Dollar Fault and corresponding increase in $k_{sn.}$
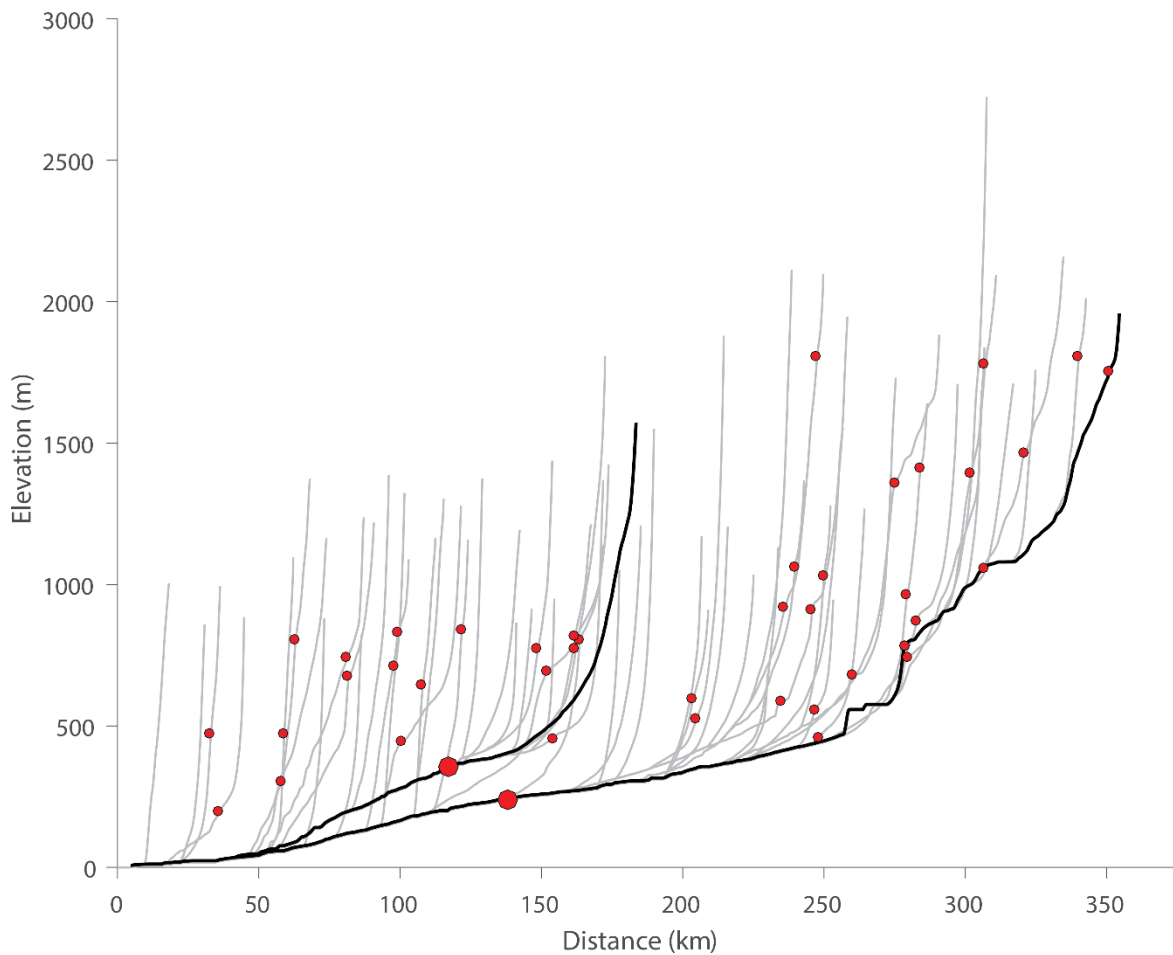
Figure 12.
Longitudinal profiles of streams included in the targeted stream profile analysis of the Rogue watershed. Heavy black lines represent the profiles of the mainstems of the Rogue (right) and Illinois (left) rivers, tributaries are represented by thin gray lines. Large red circles mark knickpoints associated with convexities in the trunk profiles of the Rogue and Illinois rivers, corresponding to where the 8 Dollar Fault crosses these channels.
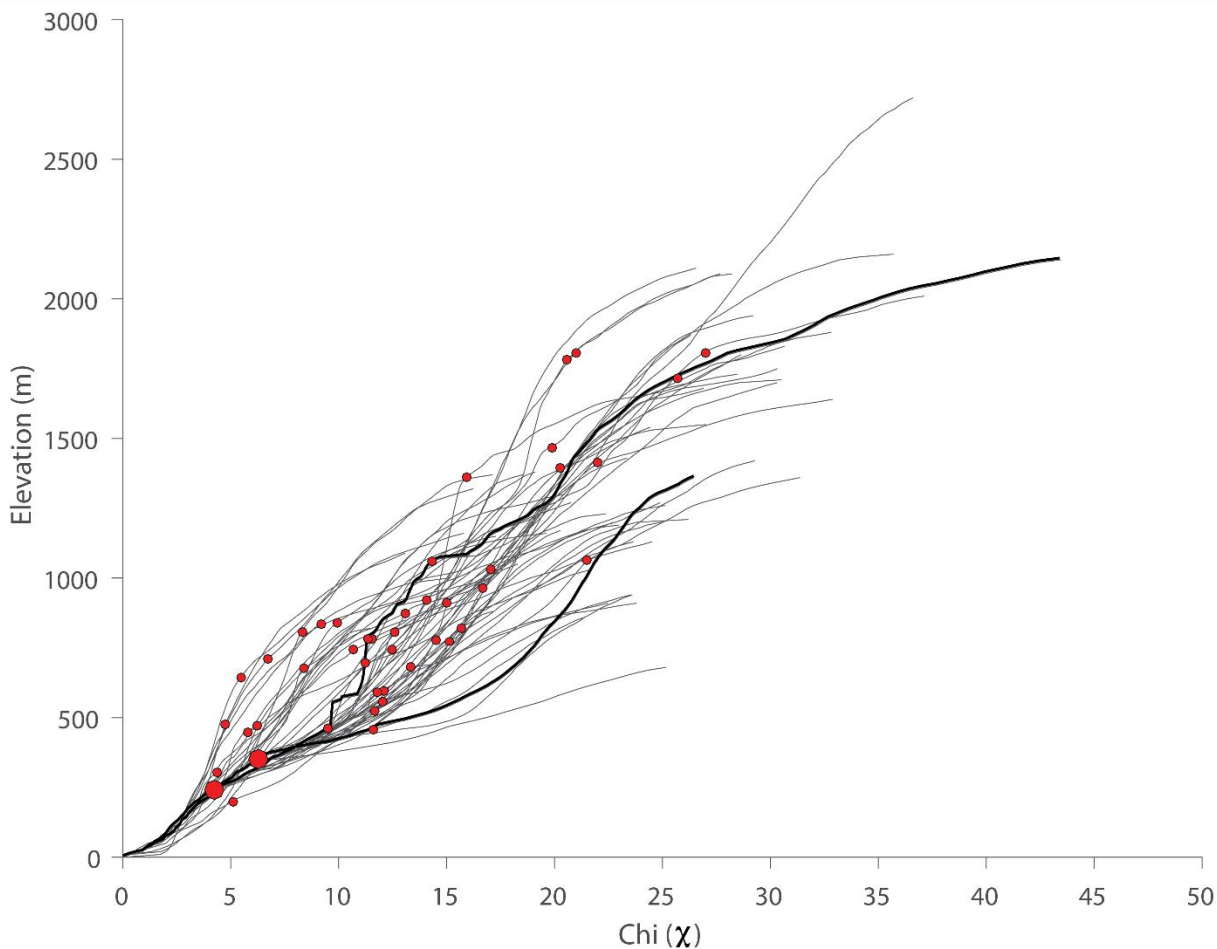
Figure 13.
Plot of chi (χ) vs elevation for the population of streams included in this stream profile analysis. Heavy black lines represent the trunk streams of the Rogue (upper) and Illinois (lower) rivers; light gray lines represent tributary streams. Large red circles mark knickpoints associated with convexities in the trunk profiles, corresponding to where the 8 Dollar Fault crosses these channels. Small circles represent knickpoints identified along tributaries to the Rogue and Illinois rivers.
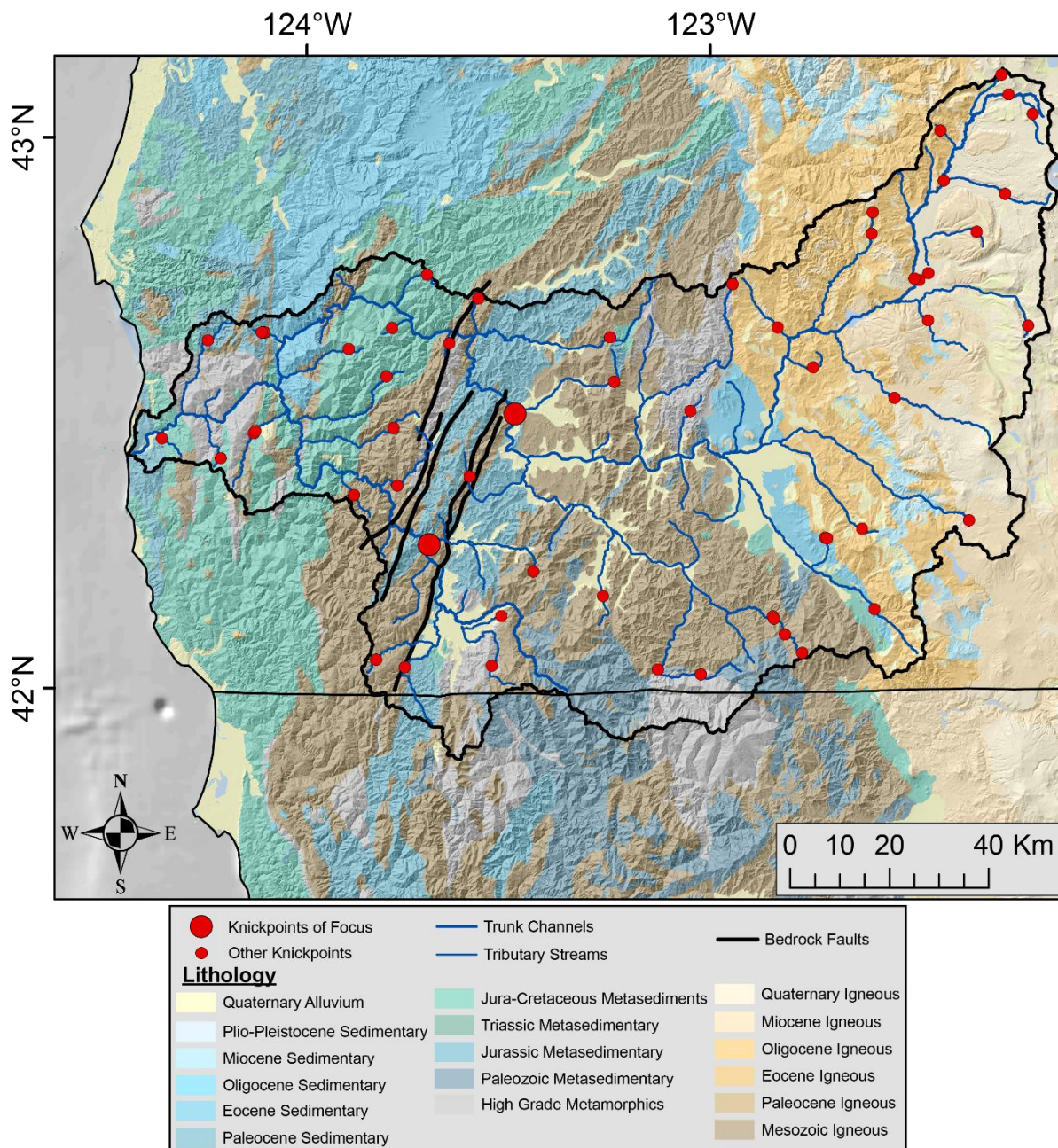
Figure 14.
Knickpoints identified from the targeted stream profile analysis laid over general geology, divided by age and general lithology. Large red circles correspond to knickzones at the head of convexities in the longitudinal profiles of the Rogue and Illinois rivers, note their proximity to the 8 Dollar Fault. Small red circles are other knickpoints identified in this analysis. Heavy blue lines identify the trunk streams of the Rogue and Illinois rivers, thin blue lines are tributaries included in the analysis, heavy black lines show faults aligned with relief, black sinuous outline marks the Rogue watershed boundary.
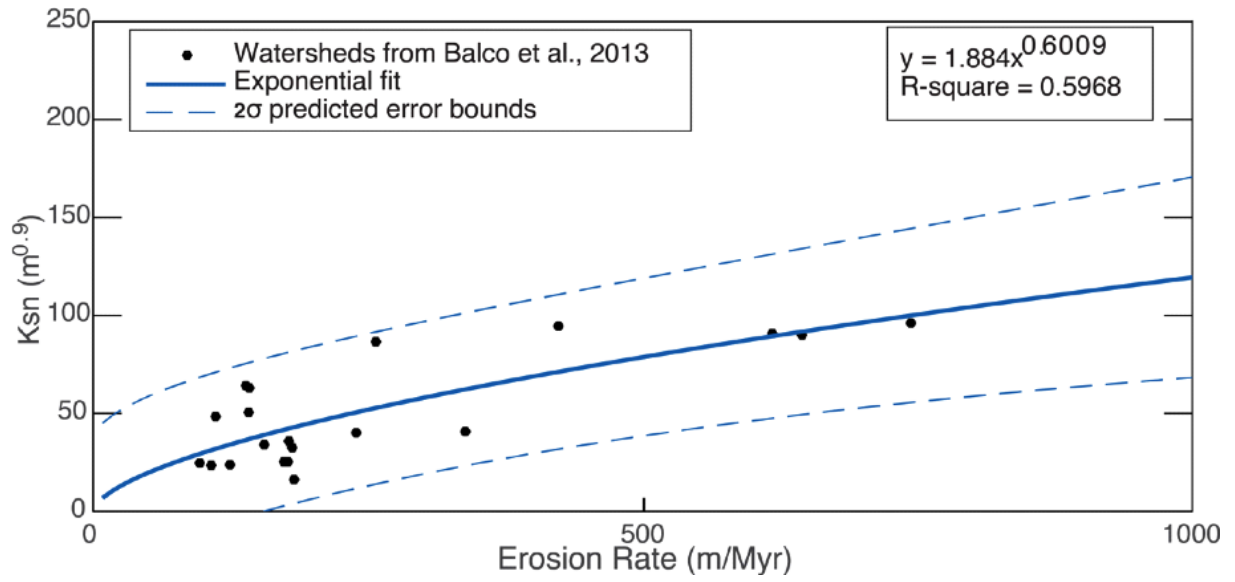
Figure 15.
Power law fit relating long term erosion rates (cosmogenic [10]Be) from Balco et al. (2013) to the basin averaged channel steepness (k_{sn}) calculated in this study.
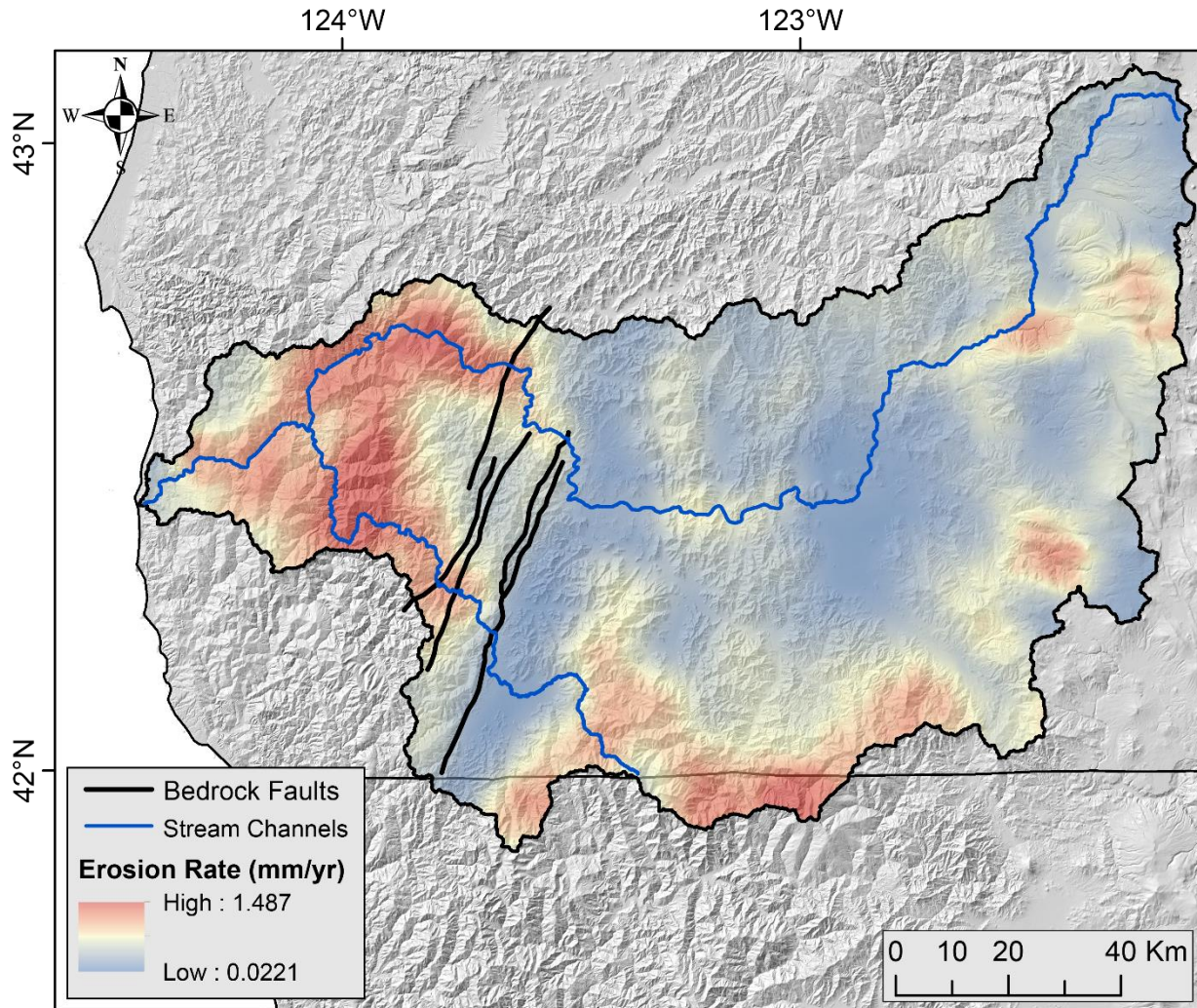
Figure 16.
Map of calibrated erosion rates across the Rogue River watershed. Erosion rates were calibrated from the interpolated grid of channel steepness (k_{sn}) for streams across the Rogue River watershed (Figures 10, 15). Erosion rates were smoothed with a 5km circular moving window to estimate spatial averages. Note the disparity in calibrated erosion rates either side of the 8 Dollar Fault.
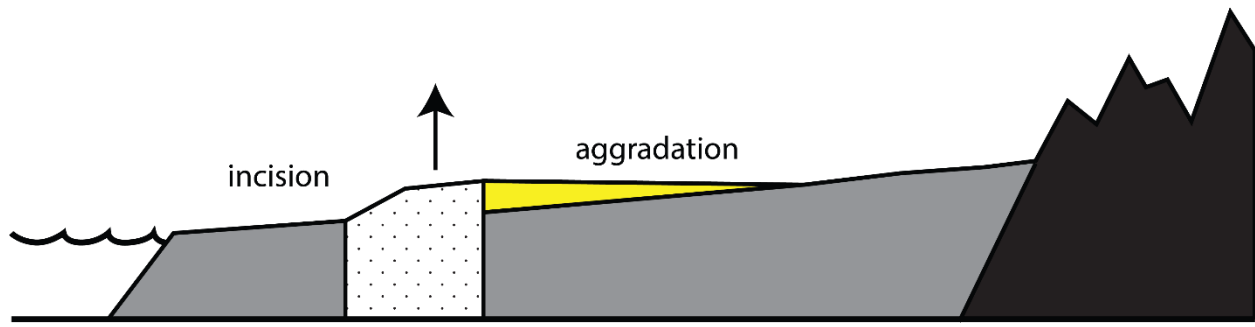
Figure 17.
Conceptual model for response of a fluvial system to an uplifting block in the center of a profile adapted from Humphrey & Konrad (2000). Aggradation of sediment and development of low relief terrain upstream of an uplifting block generating downstream incision and relief corresponds to the geomorphology of the Rogue River across the 8 Dollar Fault.

<u>Bibliography</u>

Balco, G., Finnegan, N., Gendaszek, A., Stone, J. O. H., & Thompson, A. (2013). Erosional response to northward-propagating crustal thickening in the coastal ranges of the U.S. pacific northwest. *American Journal of Science*, *313*, 790–806.

Blakely, R. J., Wells, R. E., Tolan, T. L., Beeson, M. H., Trehu, A. M., & Liberty, L. M. (2000). New aeromagnetic data reveal large strike-slip (?) faults in the northern Willamette Valley, Oregon. *Geological Society of America Bulletin*, *112*(8), 1225-1233.

Blakely, R. J., Wells, R. E., Weaver, C. S., & Johnson, S. Y. (2002). Location, structure, and seismicity of the Seattle fault zone, Washington: Evidence from aeromagnetic anomalies, geologic mapping, and seismic-reflection data. *Geological Society of America Bulletin*, *114*(2), 169-177.

Brooks, H. C., & Ramp, L. (1968). Gold and silver in Oregon. *Oregon Department of Geology and Mineral Industries Bulletin 61*, 349 p.

Brudzinski, M. R., & Allen, R. M. (2007). Segmentation in episodic tremor and slip all along Cascadia. *Geology*, *35*(10), 907–910.

Burgette, R. J., Weldon, R. J., & Schmidt, D. A. (2009). Interseismic uplift rates for western Oregon and along-strike variation in locking on the Cascadia subduction zone. *Journal of Geophysical Research: Solid Earth*, *114*(1), 1–24.

Crosby, B. T., & Whipple, K. X. (2006). Knickpoint initiation and distribution within fluvial

    networks: 236 waterfalls in the Waipaoa River, North Island, New

    Zealand. *Geomorphology*, *82*(1-2), 16-38.

Delano, J. E., Amos, C. B., Loveless, J. P., Rittenour, T. M., Sherrod, B. L., & Lynch, E. M.

    (2017). Influence of the megathrust earthquake cycle on upper-plate deformation in the

    Cascadia forearc of Washington State, USA. *Geology*, *45*(11), 1051-1054.

DiBiase, R. A., & Whipple, K. X. (2011). The influence of erosion thresholds and runoff

    variability on the relationships among topography, climate, and erosion rate. *Journal of*

    Geophysical Research: Earth Surface, *116*(F4).

Duvall, A., Kirby, E., & Burbank, D. (2004). Tectonic and lithologic controls on bedrock

    channel profiles and processes in coastal California. *Journal of Geophysical Research:*

    Earth Surface, *109*(F3).

Flint, J. J. (1974). Stream gradient as a function of order, magnitude, and discharge. *Water*

    Resources Research, *10*(5), 969-973.

Forte, A. M., Yanites, B. J., & Whipple, K. X. (2016). Complexities of landscape evolution

    during incision through layered stratigraphy with contrasts in rock strength. *Earth Surface*

    Processes and Landforms, *41*(12), 1736-1757.

Furlong, K. P., & Govers, R. (1999). Ephemeral crustal thickening at a triple junction: The

    Mendocino crustal conveyor. *Geology*, *27*(2), 127–130.

Hack, J.T. (1957). Studies of Longitudinal Stream Profiles in Virginia and Maryland. *U.S. Geological Survey Professional Paper, 294-B*, p. 97.

Harkins, N., Kirby, E., Heimsath, A., Robinson, R., & Reiser, U. (2007). Transient fluvial incision in the headwaters of the Yellow River, northeastern Tibet, China. *Journal of Geophysical Research: Earth Surface*, *112*(F3).

Heimsath, A. M., Furbish, D. J., & Dietrich, W. E. (2005). The illusion of diffusion: Field evidence for depth-dependent sediment transport. *Geology*, *33*(12), 949-952.

Heller, P. L., Peterman, Z. E., O'NEIL, J. R., & Shafiqullah, M. (1985). Isotopic provenance of sandstones from the eocene tyee formation, Oregon Coast Range. *Geological Society of America Bulletin*, *96*(6), 770-780.

Heller, P. L., Tabor, R. W., & Suczek, C. A. (1987). Paleogeographic evolution of the United States Pacific Northwest during Paleogene time. *Canadian Journal of Earth Sciences*, *24*(8), 1652-1667.

Humphrey, N. F., & Konrad, S. K. (2000). River incision or diversion in response to bedrock uplift. *Geology*, *28*(1), 43-46.

Humphreys, E. D. (1995). Post-Laramide removal of the Farallon slab, western United States. *Geology*, *23*(11), 987-990.

Irwin, W. P. (1977). Ophiolitic terranes of California, Oregon, and Nevada. *Oregon Department of Geology and Mineral Resources Bulletin*, *95*, 75-92.

Irwin, W. P. (1994). Geologic Map of the Klamath Mountains, California and Oregon. *U.S. Geological Survey Report, IMAP-2148*.

Irwin, W. P. (1997). Preliminary map of selected post-Nevadan geologic features of the Klamath

    Mountains and adjacent Area, California and Oregon. *Open-File Report 97-465*, 1–22.\

Kelsey, H. M. (1990). Late Quaternary deformation of marine terraces on the Cascadia

    subduction zone near Cape Blanco, Oregon. *Tectonics*, *9*(5), 983-1014.

Kelsey, H. M., & Bockheim, J. G. (1994). Coastal landscape evolution as a function of eustasy

    and surface uplift rate, Cascadia margin, southern Oregon. *Geological Society of America*

    Bulletin, *106*(6), 840-854.

Kelsey, H. M., Engebretson, D. C., Mitchell, C. E., & Ticknor, R. L. (1994). Topographic form

    of the Coast Ranges of the Cascadia margin in relation to coastal uplift rates and plate

    subduction. *Journal of Geophysical Research: Solid Earth*, *99*(B6), 12245-12255.

Kirby, E., & Ouimet, W. (2011). Tectonic geomorphology along the eastern margin of Tibet:

    Insights into the pattern and processes of active deformation adjacent to the Sichuan

    Basin. *Geological Society, London, Special Publications*, *353*(1), 165-188.

Kirby, E., & Whipple, K. (2001). Quantifying differential rock-uplift rates via stream profile

    analysis. *Geology*, *29*(5), 415–418.

Kirby, E., & Whipple, K. X. (2012). Expression of active tectonics in erosional landscapes.

    Journal of Structural Geology, *44*, 54–75.

Kobor, J. S., & Roering, J. J. (2004). Systematic variation of bedrock channel gradients in the

    central Oregon Coast Range: implications for rock uplift and shallow

    landsliding. *Geomorphology*, *62*(3-4), 239-256.

Lague, D., Hovius, N., & Davy, P. (2005). Discharge, discharge variability, and the bedrock channel profile. *Journal of Geophysical Research: Earth Surface*, *110*(F4).

Lavé, J., & Avouac, J. P. (2000). Active folding of fluvial terraces across the Siwaliks Hills, Himalayas of central Nepal. *Journal of Geophysical Research*, *105*(B3), 5735.

Lock, J., Kelsey, H., Furlong, K., & Woolace, A. (2006). Late Neogene and Quaternary landscape evolution of the northern California Coast Ranges: Evidence for Mendocino triple junction tectonics. *Bulletin of the Geological Society of America*, *118*(9–10), 1232–1246.

McInelly, G. W., & Kelsey, H. M. (1990). Late Quaternary tectonic deformation in the Cape Arago-Bandon region of coastal Oregon as deduced from wave-cut platforms. *Journal of Geophysical Research: Solid Earth*, *95*(B5), 6699-6713.

McKnight, B. K. (1984). Stratigraphy and sedimentology of the Payne Cliffs Formation, southwestern Oregon. *Pacific Section S.E.P.M.*, Vol. 42, p. 187 – 194.

McNutt, M. K. (1983). Influence of plate subduction on isostatic compensation in northern California. *Tectonics*, *2*(4), 399-415.

Meigs, A., & Waldien, T. (2013). Shear development and overprinting in a back-arc basin, Klamath Falls, Oregon.

Merritts, D. J., Vincent, K. R., & Wohl, E. E. (1994). Long river profiles, tectonism, and eustasy: A guide to interpreting fluvial terraces. *Journal of Geophysical Research*, *99*(B7), 14031–14050.

Molnar, P., & England, P. (1990). Late Cenozoic uplift of mountain ranges and global climate

 change: chicken or egg?. *Nature*, *346*(6279), 29-34.

Morell, K. D., Regalla, C., Leonard, L. J., Amos, C., & Levson, V. (2017). Quaternary Rupture

 of a Crustal Fault beneath Victoria, British Columbia, Canada. *GSA Today*, *27*(3).

Mudd, S. M., Attal, M., Milodowski, D. T., Grieve, S., & Valters, D. A. (2014) A statistical

 framework to quantify spatial variation in channel gradients using the integral method of

 channel profile analysis. *Journal of Geophysical Research: Earth Surface, 119*(2), 138-152.

Nelson, A. R., Johnson, S. Y., Kelsey, H. M., Wells, R. E., Sherrod, B. L., Pezzopane, S. K., ...

 & Bucknam, R. C. (2003). Late Holocene earthquakes on the Toe Jam Hill fault, Seattle

 fault zone, Bainbridge Island, Washington. *Geological Society of America

 Bulletin*, *115*(11), 1388-1403.

Niemann, J. D., Gasparini, N. M., Tucker, G. E., & Bras, R. L. (2001). A quantitative evaluation

 of playfair's law and its use in testing long-term stream erosion models. *Earth Surface

 Processes and Landforms*, *26*(12), 1317–1332.

Nilsen, T. H. (1984). Oligocene tectonics and sedimentation, California. *Sedimentary

 geology*, *38*(1-4), 305-336.

Nilsen, T. H. (1984). Tectonics and sedimentation of the upper Cretaceous Hornbrook

 Formation, Oregon and California. *Pacific Section S.E.P.M.,* Vol. 38. P. 101-118.

O'Connor, J. E., Mangano, J. F., Anderson, S. W., Wallick, J. R., Jones, K. L., & Keith, M. K.

 (2014). Geologic and physiographic controls on bed-material yield, transport, and channel

morphology for alluvial and bedrock rivers, western Oregon. *Bulletin of the Geological Society of America*, *126*(X), 377–397.

OGDC-6, Oregon Geologic Data Compilation, release 6, compiled by Rachel L. Smith and Warren P. Roe.

Ouimet, W. B., Whipple, K. X., & Granger, D. E. (2009). Beyond threshold hillslopes: Channel adjustment to base-level fall in tectonically active mountain ranges. *Geology*, *37*(7), 579-582.

Perron, J. T., & Royden, L. (2013). An integral approach to bedrock river profile analysis. *Earth Surface Processes and Landforms*, *38*(6), 570–576.

Piotraschke, R., Cashman, S. M., Furlong, K. P., Kamp, P. J. J., Danišík, M., & Xu, G. (2015). Unroofing the Klamaths—Blame it on Siletzia? *Lithosphere*, *7*(4), 427–440.

PRISM Climate Group, Oregon State University, http://prism.oregonstate.edu, created 4 Feb 2004.

Raymo, M. E., & Ruddiman, W. F. (1992). Tectonic forcing of late Cenozoic climate. *Nature*, *359*(6391), 117.

Reneau, S. L., & Dietrich, W. E. (1991). Erosion rates in the southern oregon coast range: Evidence for an equilibrium between hillslope erosion and sediment yield. *Earth Surface Processes and Landforms*, *16*, 307–322.

Rosenbloom, N. A., & Anderson, R. S. (1994). Hillslope and channel evolution in a marine terraced landscape, Santa Cruz, California. *Journal of Geophysical Research: Solid Earth*, *99*(B7), 14013-14029.

Schwanghart, W., & Scherler, D. (2014). TopoToolbox 2 – MATLAB-based software for topographic analysis and modeling in Earth surface sciences. Earth Surface Dynamics, 2, 1 - 7.

Schweickert, R. A., & Irwin, P. (1989). Extensional faulting in southern Klamath Mountains, California. *Tectonics*, *8*(1), 135–149.

Simms, A. R., Rouby, H., & Lambeck, K. (2016). Marine terraces and rates of vertical tectonic motion: The importance of glacio-isostatic adjustment along the Pacific coast of central North America. *Bulletin*, *128*(1-2), 81-93.

Sliter, W. V. (1984). Foraminifers from Cretaceous limestone of the Franciscan Complex, northern California. *Pacific Section S.E.P.M.*, Vol. 43. P. 149 – 162.

Snoke, A. W., & Barnes, C. G. (2006). The development of tectonic concepts for the Klamath Mountains province, California and Oregon. *SPECIAL PAPERS-GEOLOGICAL SOCIETY OF AMERICA*, *410*, 1.

Snyder, N. P., Whipple, K. X., Tucker, G. E., & Merritts, D. J. (2000). Landscape response to tectonic forcing: Digital elevation model analysis of stream profiles in the Mendocino triple junction region, northern California. *Geological Society of America Bulletin*, *112*(8), 1250-1263.

Snyder, N. P., Whipple, K. X., Tucker, G. E., & Merritts, D. J. (2003). Importance of a stochastic
distribution of floods and erosion thresholds in the bedrock river incision problem. *Journal
of Geophysical Research: Solid Earth*, *108*(B2).

Speth, G. T., Amos, C. B., Amidon, W. H., Balco, G., Meigs, A. J., & Graf, S. (2018). Glacial
chronology and slip rate on the west Klamath Lake fault zone, Oregon. *Geological Society
of America Bulletin*.

Trehu, A. M., Asudeh, I., Brocher, T. M., Luetgert, J. H., Mooney, W. D., Nabelek, J. L., &
Nakamura, Y. (1994). Crustal architecture of the Cascadia forearc. *Science*, *266*(5183), 237-
243.

U.S. Geological Survey, 2016, National Water Information System data available on the World
Wide Web (USGS Water Data for the Nation), accessed November 10, 2017, at URL
https://nwis.waterdata.usgs.gov/or/nwis/peak?site_no=14361500&agency_cd=USGS&form
at=html.

U.S. Geological Survey and California Geological Survey, 2006, Quaternary fault and fold
database for the United States: http//earthquake.usgs.gov/hazards/qfaults/ (January 2016).

VanLaningham, S., Meigs, A., & Goldfinger, C. (2006). The effects of rock uplift and rock
resistance on river morphology in a subduction zone forearc, Oregon, USA. *Earth Surface
Processes and Landforms*, *31*(10), 1257–1279.

Wells, R. E., Weaver, C. S., & Blakely, R. J. (1998). Fore-arc migration in Cascadia and its
neotectonic significance. *Geology*, *26*(8), 759-762.

Wells, R. E., & Simpson, R. W. (2001). Northward migration of the Cascadia forearc in the
northwestern US and implications for subduction deformation. *Earth, Planets and
Space*, *53*(4), 275-283.

Wells, R. E., Friedman, R., Pyle, D., Duncan, R., & Haeussler, P., W. J. (2014). Geologic history
of Siletzia, a large igneous province in the Oregon and Washington Coast Range:
Correlation to the geomagnetic polarity time scale and implications for a long-lived
Yellowstone hotspot. *Geosphere*, *10*(4), 692.

Willett, S. D. (1999). Orogeny and orography: The effects of erosion on the structure of
mountain belts. *Journal of Geophysical Research: Solid Earth*, *104*(B12), 28957-28981.

Willett, S. D., & Brandon, M. T. (2002). On steady states in mountain belts. *Geology*, *30*(2),
175-178.

Wilson, D. S. (2002). The Juan de Fuca plate and slab: Isochron structure and Cenozoic plate
motions. Kirby, S. H., Wang, K., and Dunlop, S. (Eds.) In *The Cascadia Subduction Zone
and Related Subduction Systems – Seismic Structure, Intraslab Earthquakes and Processes,
and Earthquake Hazards.* U.S. Geological Survey Open-File Report 02-328, 182 pp.

Whipple, K. X., Kirby, E., & Brocklehurst, S. H. (1999). Geomorphic limits to climate-induced
increases in topographic relief. *Nature*, *401*(6748), 39.

Whipple, K. X. (2004). Bedrock Rivers and the Geomorphology of Active Orogens. *Annual
Review of Earth and Planetary Sciences*, *32*(1), 151–185.

Whipple, K. X. & Tucker, G. E. (1999). Dynamics of the stream-power river incision model: Implications for height limits of mountain ranges, landscape response timescales, and research needs. *Journal of Geophysical Research*, *104*, 661–674.

Whipple, Kelin X. & Tucker, G. E. (2002). Implications of sediment-flux driven river incision models for landscape evolution. *Journal of Geophysical Research : Solid Earth*, *107*(B2), ETG-3.

Wobus, C., Whipple, K. X., Kirby, E., Snyder, N., Johnson, J., Spyropolou, K., Crosby, B., Sheehan, D., & Willett., S. D. (2006). Tectonics from topography: procedures, promise, and pitfalls. *Geological Society of America Special Paper*, *398*(4), 55–74.

Yule, J. D. (1996). *Geologic and tectonic evolution of Jurassic marginal ocean basin lithosphere, Klamath Mountains, Oregon: Pasadena, California Institute of Technology* (Doctoral dissertation, Ph. D. Dissertation, 308 p., 11 pls., scale 1: 96,000 and 1: 24,000).

Appendix I: Specific Methods

i.   Methods for Stream Profile Analysis

Stream profile analysis was conducted using the Geomorphtools toolbox shared across

ArcGIS and MATLAB platforms as described by Wobus et al. (2006). Elevation data from the

30m SRTM national elevation dataset (NED) was used for this analysis. Stream data was then

smoothed using a moving average filter and a window length of 1km.

Knickpoints were primarily identified on plots of the logarithm of slope vs the logarithm

of area (log S-log A) where channel gradients were calculated on a constant vertical interval of

10m (Wobus et al., 2006). Regressions of specific channel reaches yield data on the channel

concavity index (θ), and normalized channel steepness index (k_{sn}) allowing for analysis of

variation along a single profile. The evaluation of concavity is especially important as it provides

an evaluative measure or validation for the reference concavity (θ_{ref}) set prior to the analysis.

It is important to note that fluvial scaling relationships along a channel in log S-log A

space are generally valid below a critical contributing area (A_{cr}); in many orogens this is

approximately $A_{cr} < 1$ km^2 (e.g. Montgomery and Foufoula-Georgiou, 1993). The form of this

transition often appears as a break in slope in the log S-log A scaling relationship (Kirby and

Whipple, 2012). These observations are interpreted as a transition from a colluvial/debris-flow

dominated process region to a fluvial process dominated channel (Stock and Dieterich, 2003).

Importantly, and especially pertinent in the Oregon Coast Ranges, is the potential influence of

debris-flows on channels up to a critical area (A_{cr}) of 10 km^2 with potential implications on the

form of the channel and regional topography (Stock and Dieterich, 2003).

ii.   Methods for Erosion Rate Calibration

Building a k_{sn} grid

To generate a spatially representative grid of channel steepness indices across the region, the channel steepness (k_{sn}) was calculated for all channels in the Rogue watershed of contributing area >1 km^2. The grid was built from this network by first converting it to a raster and then passing a circular filter with a radius of 5 km over the grid.

Prior to the calibration of the channel steepness grid to the erosion rate fit, the channel steepness data was clipped to exclude reservoirs and knickpoints with $k_{sn} > 250$ (Figure 9). This is aimed to reduce the impact of local outliers on the broader pattern of channel steepness. Furthermore, when examining the locally restricted features that exhibit channel steepness >250 there are only a few primary contributors. The channels exhibiting k_{sn} >250 sit within portions of the canyons draining young volcanic rocks of the Cascade Arc, vertical steps in channel form produced by reservoirs, and tributary junctions with the mainstem in the deeply incised canyons of the lower Rogue and Illinois rivers.

Excluding knickpoints within canyons draining the Cascades is reasonable in our erosion rate extrapolation for several reasons. First, the intermittent nature of active volcanism leads to a local transient response that depends on the timing and magnitude of volcanic deposition in valleys. This transient response is not necessarily representative of rock uplift. Second, there are potential lithologic contrasts introduced between young volcanic cover and the bedrock of the Klamath terranes. Finally, because all of these knickpoints lie upstream of, and at higher elevation than, the broad knickzones along the trunk stream of the Rogue River.

Similarly, the vertical steps in channels produced by the small number of reservoirs within the Rogue watershed are excluded for the self-evident reason that these features represent are an artificial influence on the longitudinal profiles.

The nature of a few knickpoints with k_{sn} >250 in the lower Rogue River watershed is is considered separately greater likelihood that these features have tectonic or geomorphic significance. Their occurrence in the western block of the forearc is consistent with a recent increase in rock uplift rate in this region. Most of these knickpoints are localized to tributary junctions where a small or narrow tributary channel joins the main stem of the Rogue. Some of these may be artifacts of the DEM resolution; in a case where the tributary is narrow ($<$ ~30m), the elevation of the pixels near the junction may overestimate true tributary bed elevations. This issue is much less pronounced along the Rogue itself. Perhaps more importantly, the Rogue river canyon is mantled with a laterally extensive bedrock strath that is present along much of the canyon. This terrace reaches a maximum elevation of ~14m above the present river level (at mean low flow). It is likely that this terrace creates a local knickpoint in DEM analyses at tributary junctions. Thus, we exclude these from the spatial average used to create an interpolated map of channel steepness (Figure 16).

Calibrating an empirical relationship between k_{sn} and erosion rate

The channel steepness (k_{sn}) values for the watersheds corresponding to erosion rate measurements reported in Balco et al. (2013) were calculated using channel networks generated from 30m NED dataset DEMs. DEM's were prepared, channel networks extracted, and channel steepness values were calculated for each watershed using the MATLAB program package TopoToolbox (Schwanghart & Scherler, 2014).

One of the watersheds analyzed in the Balco et al. (2013) dataset exhibits an anomalously high erosion rate (~1100 m/Myr) relative to other watersheds in the Coast Ranges of Oregon and California. This river, the Van Duzen, is located in a region of recent uplift and drainage reorganization and may have lost much of its former drainage basin (Lock et al., 2013). Although the river may have already adjusted to this perturbation this system (Lock et al., 2013), the contrast between the measured erosion rate, the concentration of cosmogenic beryllium in sediment, and the modern contributing drainage area are qualitatively different than would be expected for a watershed of this size (Balco et al., 2013). In relation to the erosion rate-channel steepness scaling relationship, adding the Van Duzen data point into the fitting procedure creates a much flatter curve (higher erosion rate for a given drainage area). The result, for a channel steepness (k_{sn}) of 250, is an erosion rate of 7100 m/Myr, an erosion rate exceeding many of the highest observations made by measurements of ^{10}Be concentration in quartz globally (Portenga and Bierman, 2011). Thus, I exclude the Van Duzen river from the calibration curve (Figure 15).

APPENDIX II: INCISION RATES FROM FLUVIAL TERRACES

i.   Introduction

An initial goal of this study was to determine the spatial pattern of incision rate along the Rogue and Illinois Rivers by constraining the ages of fluvial terraces on either side of the Eight Dollar Fault. Assuming that the watershed is in long-term topographic equilibrium, differential rates of incision across the fault could be a direct proxy for differential rock uplift localized on the structure.

Field observations and mapping of fluvial terraces, discussed in Section 3, were used to determine targets for dating along the Rogue and Illinois river. Charcoal was sought on terraces ~20-25 m or less above the modern channel for dating by the radiometric ^{14}C method. Medium sands found in terrace alluvium >10 m above the modern channel were collected for dating by optically stimulated luminescence (OSL) in quartz. East of the Eight Dollar Fault, sands that constitute part of the alluvial valley fill sequence were sampled for OSL dating with the intention of constraining the transition from aggradation to incision within the valley.

The state of alluvium in terrace exposures, or in valley fill, along the Rogue and Illinois rivers varies from near pristine, loose clastic material to heavily weathered, clay-rich soil horizons. The degree of weathering and soil development expressed in outcrops of terrace alluvium varies directly with evidence of past (or ongoing) mining activities, which are ubiquitous across the region. As would be expected, it is mostly the lower terraces that are accessible in this challenging terrain; however, steep slopes, lack of access, and thick vegetation especially have made some of the higher terraces difficult to reach. In these cases, often the site conditions make it impossible to evaluate without tools and time whether there is suitable alluvium preserved for either radiocarbon or OSL dating to be employed. Furthermore, a large

number of lower straths (in some cases >10m above the channel) along both the Rogue and Illinois rivers are barren of sediment. This could be the consequence of intense placer mining that took place in the region immediately following the California gold rush (1849) and into the middle of the 20th century. Hydraulic methods were used to rapidly flush large volumes of sediment into sluice boxes where gold was separated (Brooks & Ramp, 1968).

The alternative hypothesis for strath terraces barren of fluvial sediment is that periodic, high-magnitude floods stripped the alluvial cover. Prior to dam construction in 1976, historical floods were observed to periodically reoccupy all but the highest terraces along the Rogue River. Stage heights at Grants Pass, the longest historical record in the area, record multiple events greater than 25 feet (U.S. Geological Survey, 2016). The highest flood since the installation of stream gages at Grants Pass was in 1964 and reached 34.15 feet (U.S. Geological Survey, 2016). Prior to gage installation, Army Corps of Engineers records indicate floods in 1890 and 1861 that were estimated to have reached gage heights of 36 and 43 feet respectively (U.S. Geological Survey, 2016).

The complicating effects of mining activity, high magnitude flooding, and the difficult terrain meant that the sampling campaign yielded a relatively limited set of samples (Table 2). There are a number of terraces that remain promising targets and, due to time constraints and wildfire hazards, were not reached.

ii.   Sample Collection and Analysis

As a result of terrace stripping and extensive weathering, finding alluvium that may host datable material is somewhat difficult, particularly for radiocarbon dating. Over the summer months of 2016 and 2017 charcoal (radiocarbon dating), sands (Optically Stimulated

Luminescence), quartz pebble (^{10}Be burial dating), and pisolith (oxide weathering products) samples were collected from the Rogue River and Illinois River. Samples were collected from both the valleys upstream and the canyons downstream of the Eight Dollar Fault.

A number of lower priority samples were evaluated and considered as such because of the sample sites geomorphic conditions or the fidelity of the sample itself. The stripping of terraces and weathering of alluvium have contributed to this as discussed above. However, a small number of the samples collected along the Illinois River (less so along the Rogue) were collected within what has either certainly or is likely to have been modified by large magnitude floods, debris flow activity, or large wildfires.

iii.   Discussion of High Priority Samples

Sample IR-20 is considered the highest priority sample as it is ~4.5 km northwest of the Eight Dollar Fault along the Illinois River (Figure 11). A strath terrace at this location sits 49 m above the modern Illinois River and presents an opportunity to constrain the long-term incision rate of the river in close proximity to the fault. Furthermore, sample collection went smoothly and the site conditions were favorable. The precise control on bedrock elevation, the alluvium-on-bedrock contact, and the quality of the sand deposit, being only moderately weathered and well-sorted medium sand, are all favorable for the analysis and interpretation of this sample.

Sample RR-35 [OSL] and samples from the Last Chance Mine site (RR-36 [quartz pebbles for burial dating]); RR-37 [OSL]) are considered a high priority set because of their proximity to each other (Figure 12). RR-36/RR-37 are each ~ 160m above the modern Rogue River whereas RR-35 is ~ 60m above the modern Rogue channel. The relatively large difference in elevation between sampling sites allows the comparison of incision rates over two integrated

time periods. A potential complicating factor to this benefit is that the measurements involve different analytical techniques, Be-Al burial aging of quartz pebbles for the higher sample and OSL dating of the lower sample. Obtaining an incision rate for RR-37 in addition to RR-35 would allow the evaluation of incision rate through time. Finding a significant difference in time averaged incision rate for these samples could indicate changes in hydrologic and climatic conditions or a watershed reorganization event. However, if local tectonic activity is ultimately controlling incision rate across the lower Rogue then a change in incision rate is indicating a change in rock uplift rate.

In addition, the higher, burial age target sample from the Last Chance Mine is of additional interest as existing mapping and geologic discussion stemming from a primarily economic perspective has hypothesized that this gravel deposit is coeval and potentially genetically related to Tertiary gravel deposits in the Illinois River Valley (Brooks & Ramp, 1968). The longitudinal orientation of the deposit coincidentally lends itself to this hypothesis but is otherwise entirely speculative; the intuitive and most likely relationship is that this deposit is genetically linked to the main trunk of the Rogue River. An age and incision rate incompatible with others in the Rogue watershed may suggest an affinity to the Illinois, which would have important implications for the hydrologic evolution of the watershed. However, being that the Rogue River Valley is topographically lower than the Illinois River Valley, this genetic relationship would yield a greater incision rate and imply a greater fault offset, a valuable measurement to make in either scenario.

Sample RR-33 is a high priority sample as it has the potential to date alluvial fill on the upstream side of the Eight Dollar Fault within the Rogue River Valley. This sample was taken from terraces below the slopes of the granitic Grants Pass pluton that fills the center of the Rogue

River Valley, thus it should be fairly quartz rich. Though the sample was taken close to the slopes of these hills, the beveled top and rounded, sorted, and (massively) bedded geometry of the deposit suggest it is fluvial in nature and likely related to the main trunk of the Rogue. If this is the case, this is one of the highest surfaces in the Rogue River Valley, truncated at its margins by younger alluvial terraces that comprise the major floodplain across the valley. This has potential for illuminating the age of aggradation within the valley as well as broadly providing a maximum age for these surfaces and, thus, incision of the lower cut-in-fill terracing along the banks of the Rogue River.

Sample IR-28 is from a high priority location (Figure 13), although the sample itself is of relatively low quality. The site itself does not appear to host a great amount of suitable sediment, but the degree of induration and relatively fine grain size are not ideal. The location itself has been speculated to represent alluvial infill of the Illinois River valley during the Tertiary Period (Brooks & Ramp, 1968). However, the surrounding bedrock is primarily Mesozoic age and does not provide very useful constraint for the age of the alluvial fill. A date for what appears to be the oldest alluvial fill in the valley would be an important bound on the sequence of alluvial fill. This may provide initial constraints on the beginning of infilling the Illinois River Valley.

TABLE 2.

| Sample Number	Intended Analysis	Sample Latitude	Sample Longitude	Sample Elevation (m)	Strath Elevation (m)	Channel Elevation (m)	Age (yrs)
RR-01	OSL (Quartz)	42.71359	-123.88623	124	116	103	18,640 ± 1,440
RR-01	IRSL (Feldspar)	42.71359	-123.88623	124	116	103	21,710 ± 1,750
RR-07	OSL (Quartz)	42.67313	-123.95639	96	94	67	30,030 ± 2,380
IR-20	OSL	42.268667	-123.690396	398	393	349	N/A
IR-28	OSL	42.072627	-123.650586	439		408	N/A
RR-33	OSL	42.440872	-123.43502	270		259	N/A
RR-35	OSL	42.586228	-123.58895	263	261	205	N/A
RR-37	OSL	42.581948	-123.604367	390	373	205	N/A
RR-41A/B	OSL	42.121166	-123.66856	402		400	N/A
	Cosmogenic						
RR-36	[10]Be	42.581827	-123.603792	380	373	205	N/A
RR-05	Charcoal	42.68142	-123.94404	98		71	200 ± 30
RR-08	Charcoal	42.64253	-124.03824	75		51	390 ± 30
IR-16	Charcoal	42.296898	-123.748698	331	324	315	930 ± 30
IR-27	Charcoal	42.164367	-123.651508	403	397	389	990 ± 30
IR-29	Charcoal	42.175777	-123.662768	380	380	380	930 ± 30
IR-30	Charcoal	42.176596	-123.660714	387	384	380	240 ± 30
IR-32	Charcoal	42.426567	-123.345685	283	278	268	1140 ± 30
RR-34	Charcoal	42.461802	-123.499048	278	270	250	5740 ± 30
RR-40	Charcoal	42.121085	-123.669283	400		400	110 ± 30
IR-21	Pisolith	42.257927	-123.660925	1214		368	N/A
IR-22	Pisolith	42.255983	-123.658793	1148		368	N/A
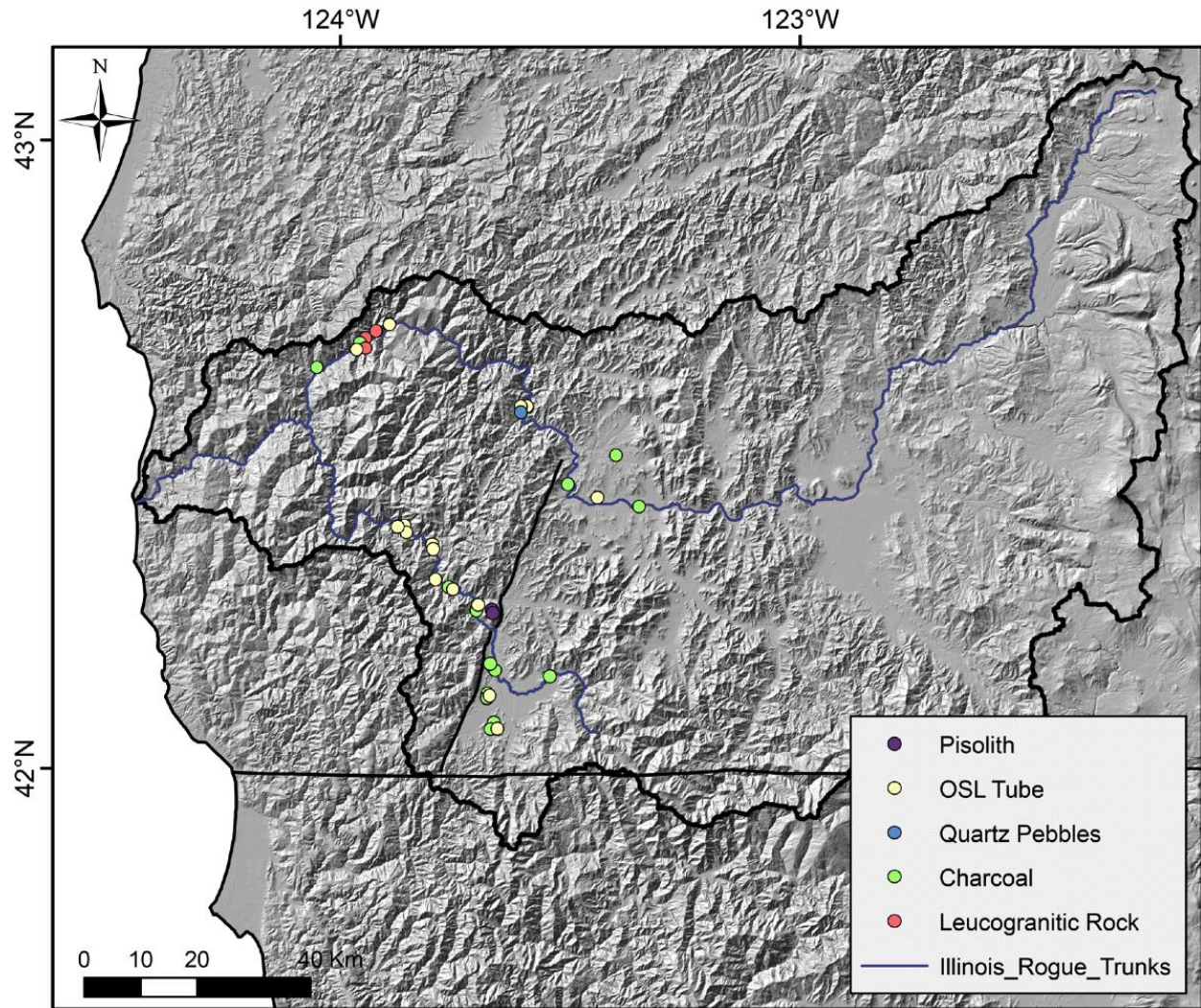
Figure 18.
Distribution of collected samples throughout the watershed. Heavy black outline is Rogue River watershed divide, blue lines are the Rogue and Illinois river trunks. Black line running across the center of the watershed represents the Eight Dollar Fault. Black boundary is the Oregon-California border.
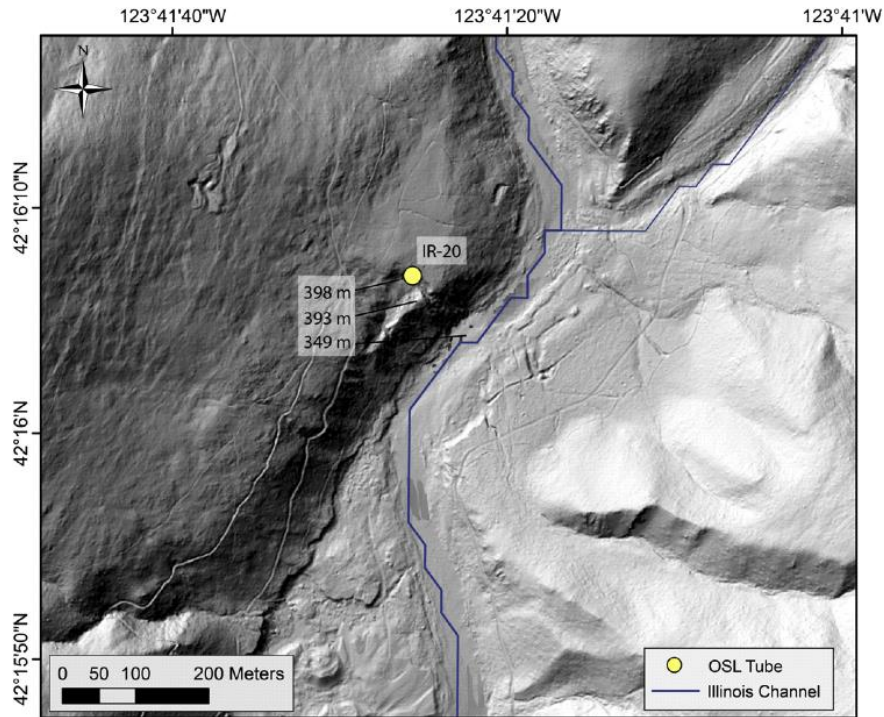
**Figure 19.
(left)**
IR-20 is a sand sample collected for (OSL) dating. Notably, the sand lens it was collected from is deposited directly on bedrock that is ~49m above the modern Illinois River channel. IR-20 is <5km linear distance west of the 8 Dollar Fault, presenting an excellent opportunity to measure an incision rate to serve as a proxy for uplift in proximity to the fault.

**Figure 20.
(right)**
Samples RR-36 and RR-37 taken at the Last Chance Mine deposit and RR-35 from the opposite side of the river provide an excellent opportunity to calculate long-term average incision rates for two periods of time along the Rogue trunk channel. Their position >20km linear distance downstream of the 8 Dollar Fault position them well to place bounds on the long-term incision rate downstream of the fault.
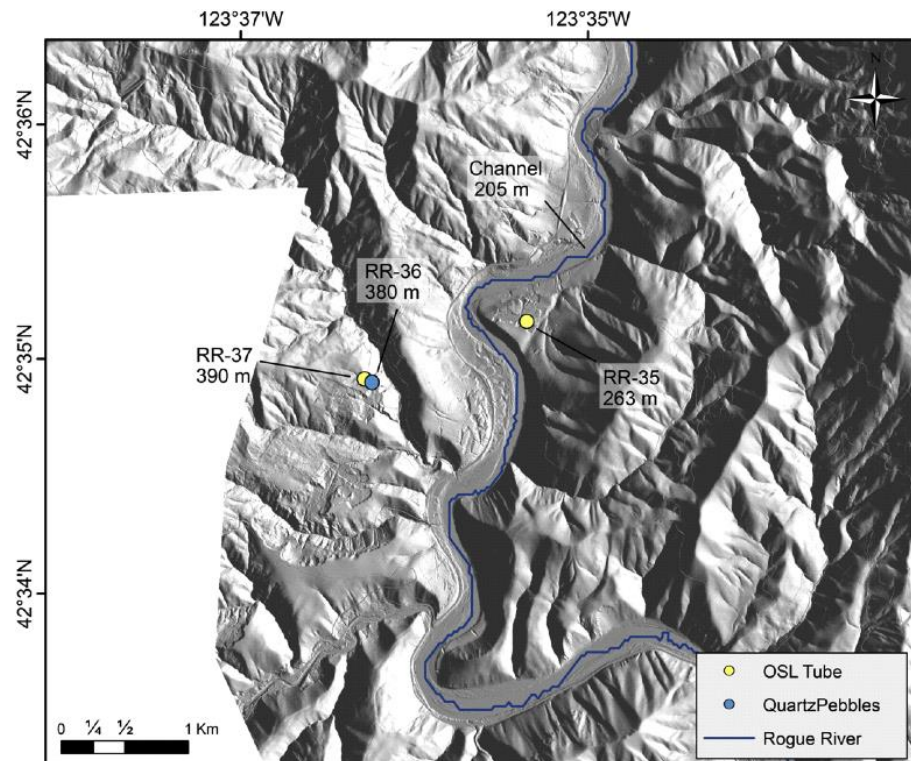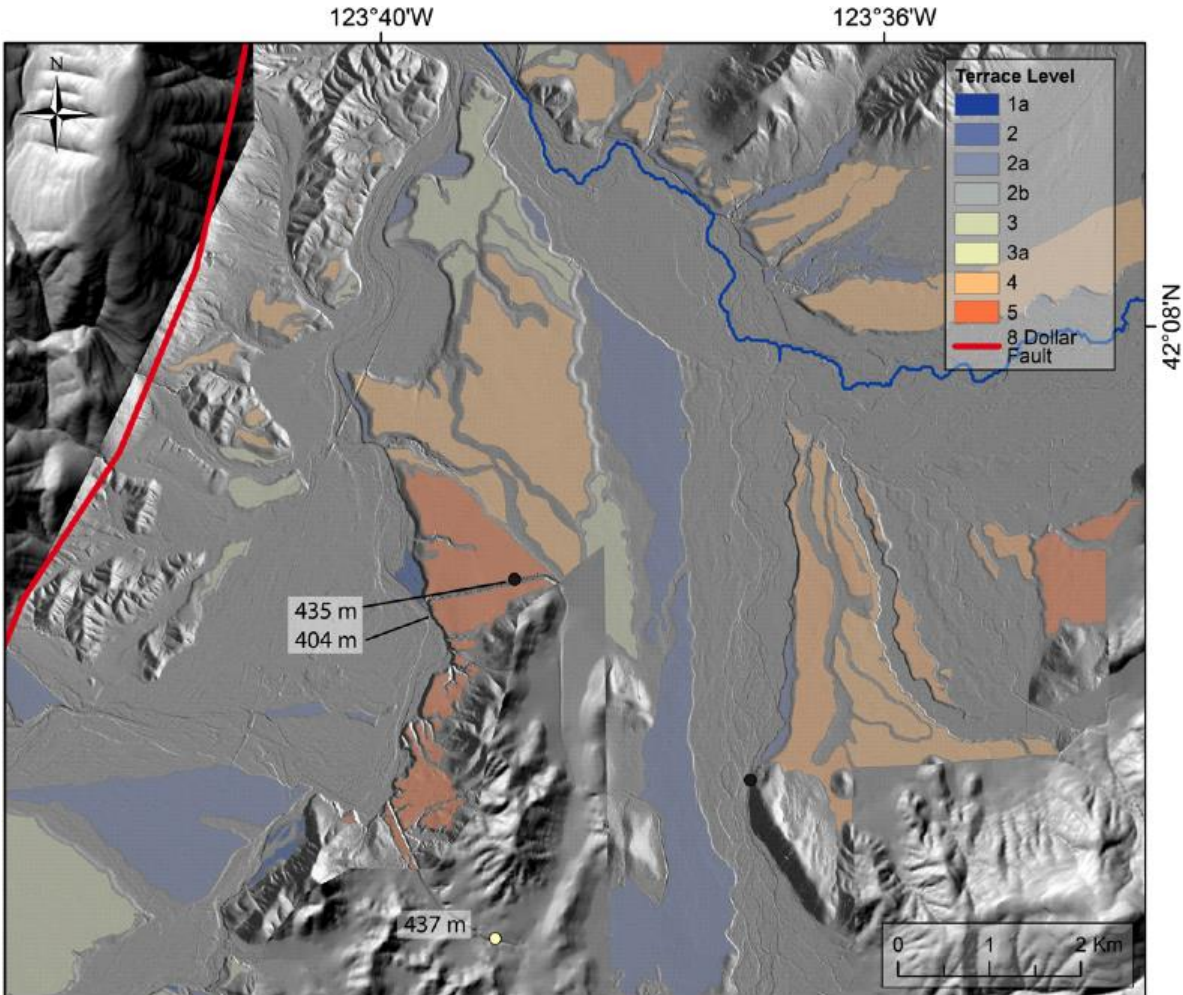
Figure 21.
Heavy red line traces the 8 Dollar Fault. The pale-yellow dot represents IR-28, a sand sample taken from heavily compacted, well indurated medium sand. This sample is likely not of very high value, due to the conditions of its collection, but the sample site is well exposed and, should more favorable material be found, is located on what has been distinguished in mining literature (Brooks & Ramp, 1968) as one of the oldest, highest elevation alluvial deposits in the Illinois River Valley. This presents an opportunity to place bounds on the cut-in-fill terrace history of the Illinois River Valley during which aggradation was driven by active deformation, likely on the 8 Dollar Fault.